Original Article

MOLECULAR METABOLISM

Exercise training reverses cancer-induced oxidative stress and decrease in muscle COPS2/TRIP15/ALIEN

Christiano R.R. Alves [1,2,3,*], Willian das Neves [1,4], Ney R. de Almeida [1], Eric J. Eichelberger [3], Paulo R. Jannig [1,5], Vanessa A. Voltarelli [1], Gabriel C. Tobias [1], Luiz R.G. Bechara [1], Daniele de Paula Faria [6], Maria J.N. Alves [7], Lars Hagen [8,9], Animesh Sharma [8,9], Geir Slupphaug [8,9], José B.N. Moreira [10], Ulrik Wisloff [10], Michael F. Hirshman [2], Carlos E. Negrão [1,7], Gilberto de Castro Jr [4], Roger Chammas [6], Kathryn J. Swoboda [3], Jorge L. Ruas [5], Laurie J. Goodyear [2], Patricia C. Brum [1,]**

ABSTRACT

Objective: We tested the hypothesis that exercise training would attenuate metabolic impairment in a model of severe cancer cachexia.
Methods: We used multiple in vivo and in vitro methods to explore the mechanisms underlying the beneficial effects induced by exercise training in tumor-bearing rats.
Results: Exercise training improved running capacity, prolonged lifespan, reduced oxidative stress, and normalized muscle mass and contractile function in tumor-bearing rats. An unbiased proteomic screening revealed COP9 signalosome complex subunit 2 (COPS2) as one of the most downregulated proteins in skeletal muscle at the early stage of cancer cachexia. Exercise training normalized muscle COPS2 protein expression in tumor-bearing rats and mice. Lung cancer patients with low endurance capacity had low muscle COPS2 protein expression as compared to age-matched control subjects. To test whether decrease in COPS2 protein levels could aggravate or be an intrinsic compensatory mechanism to protect myotubes from cancer effects, we performed experiments in vitro using primary myotubes. COPS2 knockdown in human myotubes affected multiple cellular pathways, including regulation of actin cytoskeleton. Incubation of cancer-conditioned media in mouse myotubes decreased F-actin expression, which was partially restored by COPS2 knockdown. Direct repeat 4 (DR4) response elements have been shown to positively regulate gene expression. COPS2 overexpression decreased the DR4 activity in mouse myoblasts, and COPS2 knockdown inhibited the effects of cancer-conditioned media on DR4 activity.
Conclusions: These studies demonstrated that exercise training may be an important adjuvant therapy to counteract cancer cachexia and uncovered novel mechanisms involving COPS2 to regulate myotube homeostasis in cancer cachexia.

Keywords Cancer cachexia; Muscle wasting; Atrophy; Endurance exercise; Response elements

1. INTRODUCTION

While there are multiple and complex mechanisms underlying skeletal muscle wasting, early onset of cachexia is clearly characterized by metabolic dysfunction [1—6]. Several studies have reported a disruption of muscle oxidative metabolism in cancer animal models and cancer patients, which may be the trigger for cause of muscle atrophy [1,7—15]. Disrupted oxidative metabolism induces abnormal production of reactive oxygen species that ultimately impairs protein quality control and skeletal muscle contractile capacity [16—19]. Therefore, oxidative stress seems a major regulator of muscle mass and function, and current studies are necessary to determine whether preventing disrupted oxidative metabolism at early stages would counteract muscle atrophy and weakness in cancer cachexia. Aerobic exercise training improves muscle oxidative metabolism and induces pleiotropic effects, including altered rates of blood flow, energy production, and substrate utilization [20]. Exercise training has been extensively applied as a non-pharmacological treatment for

[1]School of Physical Education and Sport, University of Sao Paulo, Sao Paulo, Brazil [2]Section on Integrative Physiology and Metabolism, Joslin Diabetes Center, Harvard Medical School, Boston, MA, USA [3]Center for Genomic Medicine, Massachusetts General Hospital, Boston, MA, USA [4]Instituto do Cancer do Estado de Sao Paulo ICESP, Hospital das Clinicas HC FMUSP, Faculdade de Medicina da Universidade de Sao Paulo, Sao Paulo, Brazil [5]Department of Physiology and Pharmacology, Karolinska Institutet, Stockholm, Sweden [6]Department of Radiology and Oncology, Faculdade de Medicina da Universidade de São Paulo, Sao Paulo, Brazil [7]Heart Institute, School of Medicine, University of Sao Paulo, Sao Paulo, Brazil [8]Department of Clinical and Molecular Medicine, Norwegian University of Science and Technology, Trondheim, Norway [9]Proteomics and Modomics Experimental Core, PROMEC, at NTNU and the Central Norway Regional Health Authority, Stjørdal, Norway [10]K.G. Jebsen Center of Exercise in Medicine at Department of Circulation and Medical Imaging, Norwegian University of Science and Technology, Trondheim, Norway

*Corresponding author. School of Physical Education and Sport, University of Sao Paulo, Sao Paulo, Brazil. E-mail: calves2@mgh.harvard.edu (C.R.R. Alves).

**Corresponding author. E-mail: topcbrum@usp.br (P.C. Brum).

Received April 28, 2020 • Accepted May 4, 2020 • Available online 11 May 2020

https://doi.org/10.1016/j.molmet.2020.101012

endocrine, cardiovascular, and neurological diseases [21–26], and recent studies have suggested that exercise training is also safe and tolerable for cancer patients during and following primary cancer therapy [27–29]. Although well-controlled studies investigating the specific effects of exercise training in advanced cancer patients are challenging because of severe fatigue and concurrent therapies, exercise training also seems to promote benefits in cancer cachexia animal models [16,30–35]. However, the molecular mechanisms underlying the beneficial effects of exercise training in cancer cachexia are poorly understood.

In our study we tested the hypothesis that exercise training would counteract metabolic impairment in a model of cancer cachexia. We first established a cancer rat model with homogeneous tumor growth and mortality rate, and we determined the effects of different exercise training protocols in this model. To explore the mechanisms underlying the effects of exercise training, we applied an unbiased mass-spectrometry-based proteomic screening in the skeletal muscle of sedentary and trained tumor-bearing rats. Our main findings indicate that COP9 signalosome complex subunit 2 (COPS2), also known as thyroid receptor interacting protein 15 (TRIP15) or ALIEN, is one of the most downregulated proteins in skeletal muscle at the early stage of cancer cachexia, and its expression is normalized by exercise training. Thus, we performed a series of *in vitro* studies to investigate the potential role of COPS2 to maintain homeostasis in muscle cells.

2. MATERIALS AND METHODS

2.1. Ethics

This study was approved by the Ethical Committee of the School of Physical Education and Sport, University of São Paulo. All animal procedures were performed in accordance with the Guidelines for the Care and Use of Laboratory Animals (National Institutes of Health, USA), and with ethical principles in animal research adopted by the Brazilian Council for the Control of Animal Experimentation. Human experiments were approved by the Ethical Committee of Instituto do Cancer do Estado de São Paulo, University of São Paulo (protocol #1.731.362) and written informed consent was obtained from all participants.

2.2. Animal models

Ten-week-old male Wistar rats and C57BL/6 mice were used in this study. The sample size used for each experiment is indicated in the figure legends. Animals were housed in an animal facility under controlled temperature (21 °C) with 12:12 h light:dark cycle and had ad libitum access to standard laboratory food and water, except for the pair-fed experiment in which the amount of food provided to a healthy control group of rats was matched daily to that consumed by the tumor-bearing experimental group. To induce bone cancer in rats, Walker 256 tumor cells were injected into the femoral cavity as previously described [36]. Suspensions of tumor cells in 5 μL of PBS were used for injection in the bone marrow. SHAM surgery was performed on the control rats. Dipyrone (Medley Farmacêutica Ltda., Brazil), an ampyrone sulfonate analgesic, was administered through the water during the entire protocol to minimize rat suffering. LLC or B16 tumor cells were injected subcutaneously in the right flank as previously described [31]. One day following tumor cell injection, mice were randomly assigned into experimental groups. Rats were euthanized by decapitation under isoflurane anesthesia and mice were euthanized by cervical dislocation under isoflurane anesthesia. For ethical purposes, rats and mice were euthanized if they appeared moribund, indicating a low probability of surviving for greater than 24 h, and were removed from the analysis.

2.3. Human studies

We recruited six male patients with histologically confirmed metastatic non-small-cell lung cancer (NSCLC). The patients were diagnosed with either squamous cell carcinoma (n = 3) or adenocarcinoma (n = 3) and were not previously treated with any cancer therapy. We also recruited 4 age- and sex-matched control subjects. All patients with NSCLC and the control subjects were tobacco smokers. This is a subcohort of study NCT03960034 registered on clinicaltrial.gov. Inclusion criteria included a) advanced stage IVa or IVb histologically-proven patients with NSCLC; b) Eastern Cooperative Oncology Group Performance status 0–2 treatment-naïve; c) current smokers or ex-smokers; d) normal renal, hepatic, and hematological functions; e) ability to perform the physical functional tests; and f) ability to to read and sign the consent form. Exclusion criteria included a) any previous systemic treatment for metastatic disease, and b) diagnosis of tumor driver mutation (*e.g.*, epidermal growth factor receptor, anaplastic lymphoma kinase). Medications in use in this cohort included Metformin (1 patient and 1 control subject), Enalapril (1 patient), Dimenhydrinate (1 patient), Losartan potassium (1 patient and 1 control), Tandrilax (1 patient), and Dipyrone (1 patient). To provide proof-of-concept, we included only cancer patients in pre-cachexia stages because our proteomic screening from tumor-bearing rats was performed in an early stage of cachexia before an established muscle wasting condition. This allowed us to apply physical tests to determine the VO2 peak and muscle biopsies for further immunoblot assay. Patients with NSCLC had lower hemoglobin levels and higher albumin levels than control subjects, as shown in Table S4. No cases with anorexia were included in this study and patients with NSCLC and control subjects had similar food intake. Cardiopulmonary exercise testing was conducted to determine VO_2peak as previously described [82]. Percutaneous muscle biopsies were obtained from the *vastus lateralis* muscle using a 5-mm modified Allendale-Bergstrom needle [82]. Local anesthesia with 1–2 mL of lidocaine 2% solution was performed. Muscle samples were immediately frozen in liquid nitrogen and subsequently stored at −80 °C. Exercise testing and muscle biopsy procedures were performed during the same week, with an interval of at least 3 days between each procedure. The experiments were conducted at the Instituto do Cancer do Estado de São Paulo and Instituto do Coração, HCFMUSP, São Paulo, Brazil.

2.4. Cell culture

Human skeletal myoblasts (Thermo Fisher Scientific; A11440) were differentiated into myotubes in Dulbecco's modified Eagle's medium (DMEM; Gibco) supplemented with 2% horse serum and 1% pen/strep. Primary mouse myoblasts were isolated and differentiated into myotubes as previously described [83,84]. C2C12, HeLa, B16, and LLC cells were cultured in DMEM supplemented with 10% fetal bovine serum and 1% pen/strep. To collect conditioned media, HeLa, B16, and LLC cells were plated at 50% confluency and incubated in DMEM serum-free media for 24 h. For incubation in myotubes, cell-conditioned media were mixed with fresh media (ratio 1:1) and supplemented with 5% horse serum (or 2% for C2C12 experiments). Primary mouse myoblast-derived myotubes were incubated with conditioned media for 12 h, 24 h, 36 h, or 48 h depending on each specific readout. Myotubes were washed with saline before protein or RNA extractions. Oxygen consumption rates (OCR) and extracellular acidification rates (ECAR) were measured in myotubes using extracellular flux analysis (XF96, Agilent Seahorse, MA USA) in sodium

bicarbonate-free DMEM supplemented with 31.7 mM NaCl, 10 mM glucose, and 2 mM glutamax (pH 7.4 adjusted using NaOH) as previously described [85]. MitoTracker Red (Thermo Fisher Scientific; M7512) was used to stain mitochondria in live myotubes according to the manufacturer's instructions. To overexpress COPS2, mouse myotubes were transduced with adenoviruses (MOI 100) expressing GFP or mouse COPS2 (ADV-255916; Vector Biolabs, Malvern, PA, USA). Twelve hours after transduction, the medium was replaced with fresh differentiation medium. To knockdown COPS2, specific siRNA sequences (Thermo Fisher Scientific) were used for human (AM16708; Assay ID 140004) or mouse (AM16708; Assay ID 161305) cells using Lipofectamine RNAiMAX Transfection Reagent (Thermo Fisher Scientific; 13778-075) in Opti-MEM Media (Thermo Fisher Scientific; 31985062). Transfections with scramble siRNA (4390843) were used for the control groups. For experiments involving adenovirus transduction or siRNA transfection in C2C12 myoblasts, media was replaced with DMEM supplemented with 2% horse serum and 1% Pen/Strep to avoid additional cell growth. All cells used in this study were maintained at 37 °C in 5% CO2.

2.5. Running capacity and exercise training protocols for mice and rats

Rats and mice were subjected to a maximum incremental running test as previously described [63]. The maximum speed achieved by each animal was recorded. Tumor cells or control solution were injected two days after the maximum incremental running test. Exercise training protocols started one day following injection and were comprised of daily treadmill running sessions for 10 consecutive days. Each aerobic interval training session consisted of 3 bouts at 85% of maximum speed for 4 min with intervals at 60% of maximum speed for 3 min. Animals in the aerobic continuous training protocol ran at 60% of maximum speed, and the duration was adjusted to match the total volume of the aerobic interval training sessions, resulting in the same total running distance between aerobic interval and continuous training [31,54]. Running speed was adjusted as cachexia progressed to maintain the relative exercise intensity (% of max running speed) throughout the study. Running speed was reduced by 20% when the animal failed to exercise at the target intensity. The same reduced intensity was then applied from the onset of the next session. Most of the rats injected with Walker 256 tumor cells had exercise intensities reduced between the 8th and 10th day post-injection (dpi).

2.6. Ex vivo skeletal muscle contractility

Contractile capacity of the extensor digitorum longus (EDL) muscle was measured. The EDL was carefully harvested and immediately used for *ex vivo* experiments. The muscles were mounted between force transducers in a tissue bath containing aerated Krebs Ringer's buffer and platinum-based electrodes for electrical stimulation. Force output was recorded after successive electrical stimulation as previously described [31,63].

2.7. Circulating lactate, cytokine concentrations and insulin tolerance test

Serum lactate and plasma glucose were determined using spectrophotometric techniques [86]. IL-1β, IL-6, IL-10, and TNF-α concentrations were determined from the serum and protein extracted from *plantaris* muscle using the Milliplex Map, rat cytokine/chemokine magnetic bead panel (Millipore, Sigma, Switzerland) according to the manufacturer's instructions. To test insulin tolerance, rats were fasted for 6 h and administered insulin (0.75 units/kg body weight) by intraperitoneal injection. Blood samples were collected to measure plasma glucose concentration at specified time points after injection.

2.8. Glutathione redox status, citrate synthase and catalase activities

Glutathione levels were measured with the Glutathione Fluorescent Detection Kit (K006-F5; Arbor Assay, USA). To block free GSH, 2-Vinylpyridine (2VP) was used according to the manufacturer's instructions. Citrate synthase activity was determined using the Citrate Synthase Assay Kit (CS 0720, Sigma–Aldrich, USA). Catalase activity was determined by the hydrogen peroxide (H_2O_2) decomposition, which was assessed by following the decay in sample absorbance at 240 nm in the presence of 10 mM H_2O_2.

2.9. Protein carbonyls, dihydroethidium fluorescence staining and lipid hydroperoxides

Protein carbonyls were assessed with the OxyBlot Protein Detection Kit (S7150; Millipore, Switzerland). Soluble proteins (20 μg) were denatured by SDS and derivatized by Dinitrophenylhydrazine (DNPH). Proteins were subjected to electrophoresis and immunoblotting according to the manufacturer's instructions. For dihydroethidium (DHE) fluorescence staining, muscle cross-sections (10 μm) were incubated with DHE (5 μM) in a light-protected incubator at 37 °C for 30 min. The sections were washed with phosphate buffered saline and fluorescence was assessed by confocal microscopy. Quantitative analysis of fluorescent images was performed with ImageJ (NIH, USA). Lipid hydroperoxides were evaluated using the modified ferrous oxidationxylenol (FOX) orange technique [65], and malondialdehyde (MDA) and 4-hydroxyalkenals (HAE) were assessed using an ALDetect Lipid Peroxidation Assay Kit (Enzo Life Sciences International, NY, USA).

2.10. Proteasome activity

26 S proteasome activity was measured by using a substrate for proteasome chymotrypsin-like catalytic site (Suc LLVY-AMC, Enzo Life Sciences, USA) as previously described [87]. Fluorescent product formation was followed in the presence or absence of epoxomicin (20 μM), a highly specific inhibitor of chymotrypsin-like proteasome activity, and the difference between the two rates was considered 26 S proteasomal activity.

2.11. Gel free proteomics and mass spectrometry analysis

Plantaris muscle extracts were homogenized in degassed 2D buffer (7 M Urea, 2 M Thiourea, 2.5% CHAPS) without DTT (dithiothreitol) at pH 5.0. Protein (600 μg) was precipitated in methanol (4 V), chloroform (1 V), and H2O (3 V) and frozen for further labeling to proceed with gel-free proteomics. Each sample was digested with trypsin and purified and analyzed by mass spectrometry. For gel-free proteomics in the Walker rat model muscle samples, technical duplicates were performed for each of the 5 biological independent biological samples. For gel-free proteomics in B16 mouse model samples, technical duplicates were performed in a pool of 8 samples in each experiment. Peptides were analyzed on an LC-MS/MS platform consisting of an Easy-nLC 1000 UHPLC system (Thermo Fisher Scientific Inc, USA) interfaced with an LTQ-Orbitrap Elite hybrid mass spectrometer (Thermo Fisher Scientific Inc, USA) via a nanospray ESI ion source (Proxeon, Odense, Denmark) as previously described [38].

Raw data files were analyzed in Proteome Discoverer 1.4 (Thermo Fisher Scientific Inc., US) using the SEQUEST HT search engine with the December 2013 version of the rat protein sequence database from UniProt (UniProt Consortium). The enzyme specified as trypsin with a

maximum of two allowed missed cleavages was searched. Precursor mass tolerance was 10 ppm and fragment mass tolerance was 0.6 Da. The Percolator tool was used for peptide validation and a cutoff value of 0.01 was used for false discovery rate. Only peptides with high confidence were used for final protein identification. To further understand the biological relevance of the identified proteins, we performed functional enrichment analysis in the context of the Kyoto Encyclopedia of Genes and Genomes (KEGG) databases using the Enrichr43 and QIAGEN'S Ingenuity Pathway Analysis (IPA).

The mass spectrometry (MS) proteomics data have been deposited into the ProteomeXchange Consortium via the PRIDE partner repository with the dataset identifier PXD013226 [88]. Proteins were quantified by processing MS data using Max Quant [89]. Preview 2.3.5 [Protein Metrics Inc.] was used to inspect the raw data to determine the optimal search criteria [90]. Specifically, the following search parameters were used: enzyme specified as Trypsin with maximum two missed cleavages allowed; protein N-terminal acetylation, carbamidomethylation of cysteine and oxidation of methionine as dynamic post-translational modification. These were imported into MaxQuant which uses *m*/*z* and RT values to align each run against every other sample with a 2-minute window match-between-run function and a 20-minute overall sliding window using a clustering-based technique. These are further queried against the rat proteome downloaded from Uniprot (https://www.uniprot.org/proteomes/UP000002494) and MaxQuant's internal contaminants database using Andromeda built into MaxQuant. Both protein and peptide identifications FDR were set to 1% thus only peptides with high confidence and a minimum length of 7 amino acids were used for final protein group identification. Peak abundances were extracted by integrating the area under the peak curve. Each protein group abundance was normalized by the total abundance of all identified peptides for each run and protein by calculated median summing all unique and razor peptide ion abundances for each protein using a label free quantification (LFQ) algorithm [89] with minimum peptides ≥ 1. These LFQ values were log transformed with base 2.

2.12. Immunoblotting and immunofluorescence

Protein isolation and immunoblotting were performed as previously described [65,91]. Primary antibodies were incubated overnight and used to probe for COPS2/TRIP15/ALIEN using Abcam Anti-CSN2 (ab83225; not commercially available anymore) or Bethyl CSN2 antibody (Cat# A300-027 A). The c-terminal Abcam Anti-CSN2 (Cat# ab155774) was used for the specific immunofluorescence experiments in C2C12 myoblasts. *Ponceau* or GAPDH (Cell Signaling Technology, USA, 2118 S and Santa Cruz, USA, #sc-20358) were used as loading controls. Membranes were imaged using the ChemiDoc Touch System (Bio-Rad, USA) or the LI-COR Odyssey Infrared Imaging System (LI-COR, Inc., USA). To understand antibody binding in COPS2 structure, PYMOL was used where a COPS PBD file was downloaded from Unitprot and the sequence was uploaded for structural analysis. COPS2 (CSN2 subunit) was colored blue, the N-terminal was colored green and the C-terminal 62 residue sequence targeted by the Abcam antibody (Cat# ab155774) was colored red as shown in Figure S8A. Alexa Fluor™ 488 Phalloidin (Thermo Fisher Scientific; A12379) was used to stain F-actin in myotubes.

2.13. *Microarray* analyses

Human myotubes transcriptome was determined using Clariom S Assay, human (Thermo Fisher Scientific) using the Thermo Fisher Scientific facility services (Santa Clara, CA, USA). All data analysis was done in R [92], using the packages "Limma" [93] and "Oligo" [94] through Bioconductor. Affymetrix data were first normalized by using robust multi-array averages. These normalized data were then fit through a linear model. The empirical Bayes statistics for differential expression was used to calculate all statistical values. Graphs were generated using ggplot2 [95]. Microarray data were submitted to NCBI Gene Expression Omnibus (GEO) Access code: GSE151591.

2.14. Quantitative RT-qPCR

RNA was isolated from tissue using an RNA extraction kit (Direct-zol™ RNA MiniPrep, Zymo Research, Irvine, CA, USA) or RNeasy Plus Universal Kits (Qiagen, Hilden, Germany). RNA was reverse-transcribed using standard reagents (High Capacity Reverse Transcription Kits, Applied Biosystems) and cDNA was amplified with Power SYBR Green PCR master mix (Applied Biosystems), using the ABI 7900HT real-time PCR system. For each gene, mRNA expression was calculated relative to Hprt for mouse cell lines and rats, and relative to TBP for human cells. Primer sequences are provided in Table S5.

2.15. Preparation of plasmid vectors and luciferase reporter assay

Vector pGL4.10 [luc2] (Promega) was linearized by digesting with HindIII and XhoI (New England Biolabs), and was then purified using the QIA quick PCR purification kit (Qiagen 28104) Two ssDNA oligos (DR4 sequence with overhangs) were annealed to form a dsDNA oligo with specific HindIII and XhoI overhangs. The linearized vector and dsDNA oligo were ligated together using T4 DNA ligase (NEB) according to manufacturer protocol. The product was then transformed into competent cells and plated onto ampicillin agar plates. Single colonies were picked the following day and grown in LB overnight. The cells were then harvested and mini prepped with Qiaprep spin Miniprep Kit (Qiagen 27104). Purified plasmid DNA was sent for sequencing to confirm successful and correct ligation. A Dual-Luciferase Reporter Assay System (Promega) was used to determine DR4 luciferase activity (firefly) and each individual well was normalized via *Renilla* luciferase internal control.

2.16. Statistical analysis

Values are presented as mean $\pm$ standard error (SE). Individual values are also presented for *in vivo* data. Analyses were conducted using Graph Pad Prism 8 (Graph Pad Software Inc., USA). Unpaired Student's *t*-test was used to test the differences between the two experimental groups. One- or two-way analysis of variance (ANOVA) was used to compare more than two experimental groups. Whenever significant effects were found in ANOVA, Fisher's least significance difference test was used for multiple comparison purposes. A log-rank test was performed to compare survival rate. Statistical significance was set at $p < 0.05$.

3. RESULTS

3.1. Injection of Walker 256 tumor cells into the bone marrow induces severe cancer cachexia in rats

To establish a model of cancer cachexia with homogeneous tumor growth and mortality rate, we injected Wistar rats with 10^6 Walker 256 tumor cells subcutaneously in the right flank or in the bone marrow via an osteotomy in the femur [36]. We observed a more homogeneous mortality rate (Figure S1A), greater decline in the ambulation test performance (Figure S1B), and greater mechanical hyperalgesia (Figure S1C) in rats injected with tumor cells in the bone marrow than in rats injected subcutaneously in the flank. Furthermore, we observed solid tumors in all rats injected in the bone

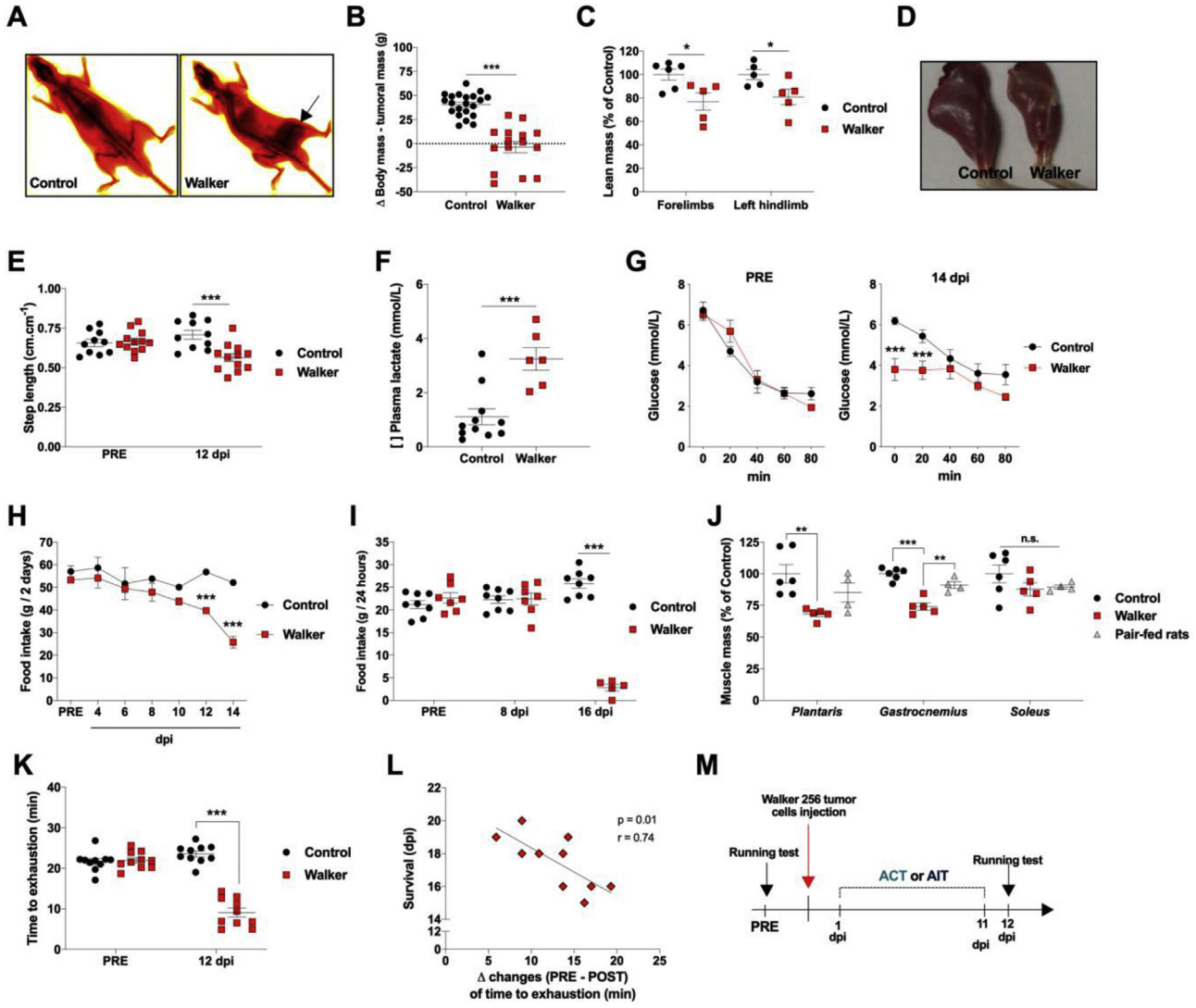

Figure 1: Bone marrow injection of Walker 256 tumor cells in rats. (**A**) Representative DXA images of Walker 256 tumor-bearing rats at 16 days post injection (dpi). (**B**) Body mass delta changes in Walker 256 tumor-bearing rats. $n = 15–21$. (**C**) Lean mass. $n = 5–6$. (**D**) Representative images of left hindlimb. (**E**) Ambulation test. $n = 10–12$. (**F**) Circulating lactate levels. $n = 6–11$. (**G**) Insulin tolerance test. $n = 6–8$. (**H**) Food intake assessed in group-housed rats. $n = 4–5$. (**I**) Food intake assessed in single-housed rats in metabolic cages. 7–8. (**J**) *Plantaris*, *Gastrocnemius,* and *Soleus* mass relative to controls. $n = 5–6$. (**K**) Running capacity. $n = 10$. (**L**) Correlation between reduced running capacity (pre–post delta change) and survival after tumor cell injection. $n = 10$. (**M**) Study design to test exercise training effects. Walker 256 tumor-bearing rats were subjected to aerobic interval (AIT) or continuous (ACT) training. Data are presented as mean ± s.e.m. $^{*}P < 0.05$; $^{**}P < 0.01$; $^{***}P < 0.001$. n.s. not significant.

marrow, while 4 of 24 of rats (16%) injected subcutaneously did not present visual tumors until 20 days post injection (dpi) and were removed from the experiment. We next injected different concentrations of tumor cells in the bone marrow and found that higher concentrations resulted in a more homogeneous mortality rate (Figure S1D). Thus, all subsequent experiments were done with rats injected in the bone marrow with 10^6 Walker 256 tumor cells, and the term "tumor-bearing rats" will be used from this point onward to refer to this model.

To further determine whether tumor-bearing rats develop cancer cachexia, we assessed changes in total and lean mass as well as in ambulation performance. Tumor-bearing rats had consistent reduction in total and lean mass (Figure 1A–D) in conjunction with a decline in the ambulation test performance (Figure 1E). Tumor-bearing rats also had higher circulating lactate concentrations (Figure 1F) and lower basal glucose levels compared with healthy control rats (Figure 1G). Tumor-bearing rats did not show changes in food intake until 10 dpi, but demonstrated a significant reduced intake starting at 12 dpi (Figure 1H,I). To investigate whether changes in the muscle mass were secondary to reduced food intake, we performed a pair-fed experiment in which the daily food intake of healthy control rats was paired to that of tumor-bearing rats. Tumor-bearing rats had decreased *plantaris* and *gastrocnemius* muscle mass, while pair-fed healthy control rats showed preserved muscle mass compared with the *ad libitum*-fed control group (Figure 1J). *Soleus* muscle mass was not affected by neither cancer nor reduced food intake (Figure 1J). Collectively, these initial findings demonstrate that Walker 256 tumor-bearing rats is a model of severe cancer cachexia with homogeneous tumor growth and mortality rate, and skeletal muscle atrophy is not only a consequence of reduced food intake.

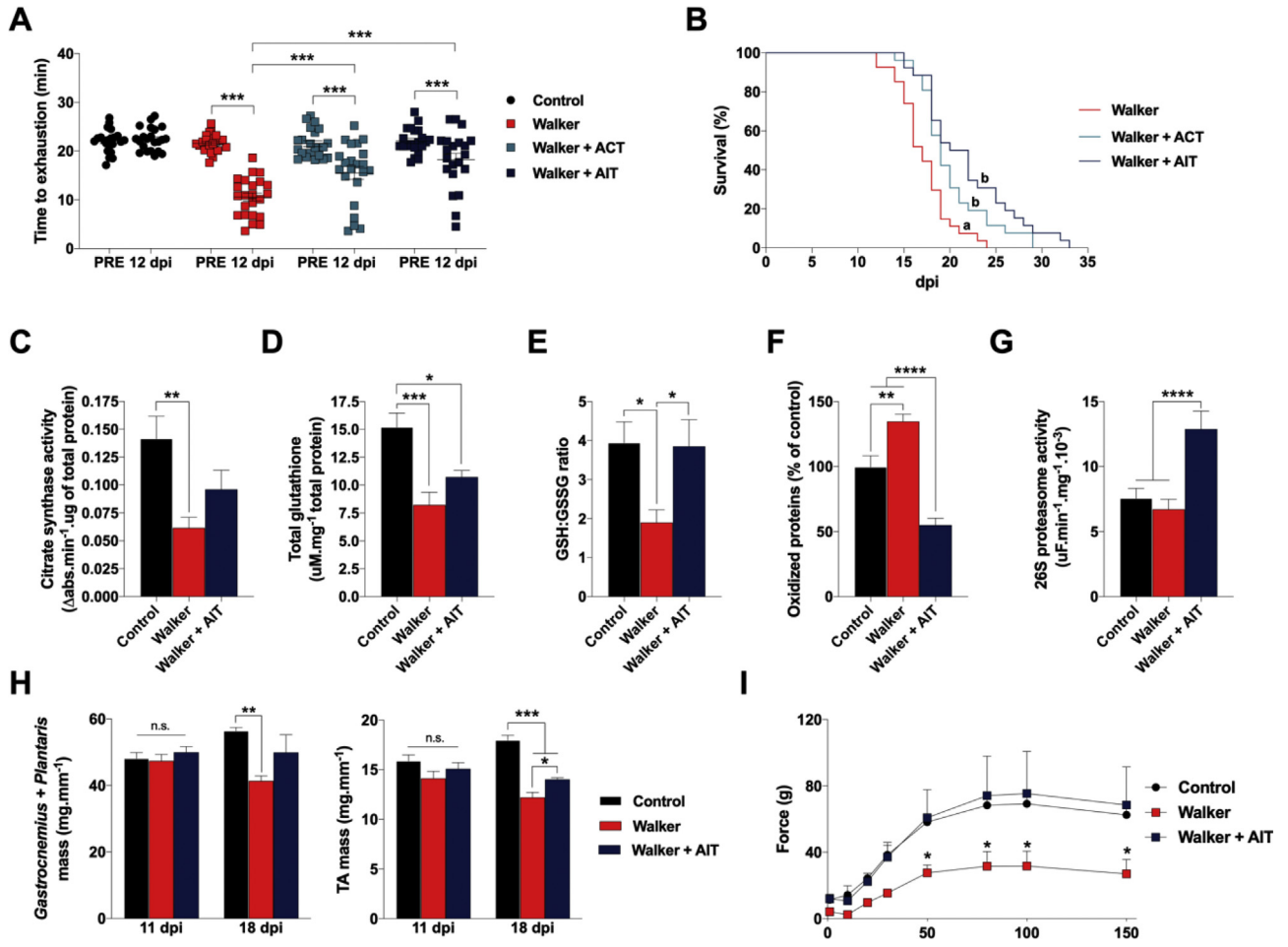

Figure 2: Effects of exercise training on running capacity, survival rate and skeletal muscle in Walker 256 tumor-bearing rats. Tumor-bearing rats were submitted to aerobic interval (AIT) or continuous (ACT) training. (**A**) Running capacity. $n = 22–23$ rats. (**B**) Survival rate. $n = 26–27$ rats. Different letters indicate significant difference between groups. (**C**) Citrate synthase activity. $n = 6–11$ rats. (**D**) Total glutathione and (**E**) ratio between reduced (GSH) and oxidized (GSSG) glutathione. $n = 6–10$ rats. (**F**) Quantification of carbonyl protein levels. $n = 6–8$ rats. (**G**) 26 S proteasome activity. $n = 6–11$ rats. (**H**) Skeletal muscle mass normalized to tibia length. $n = 4–6$ rats. (**I**) Muscle contraction capacity at 18 dpi. $n = 3$ rats. Data are presented as mean ± s.e.m. $^{*}P < 0.05$; $^{**}P < 0.01$; $^{***}P < 0.001$; $^{****}P < 0.001$. n.s. not significant. dpi: days post injection.

3.2. Exercise training improves running capacity and prolongs survival in Walker 256 tumor-bearing rats

Tumor-bearing rats had impaired running capacity (Figure 1K), which was directly correlated with time of death after tumor cell injections (Figure 1L). Therefore, the data suggest that running capacity predicts longevity in this cancer model. To test whether exercise training would improve running capacity, we subjected tumor-bearing rats to two different protocols of aerobic exercise training (interval and continuous), and we evaluated their running capacity at 12 dpi (Figure 1M). Because reduced running capacity was associated with a reduced lifespan, we also evaluated the effects of these two protocols on the mortality rate. Both aerobic interval and continuous training improved running capacity (Figure 2A) and prolonged the lifespan (Figure 2B), with no significant changes in the tumor size (Figure S2A) or circulating serum TNFα levels (Figure S2B). Additionally, tumor-bearing rats had increased wet/dry lung mass difference, a marker of lung edema [37], which was normalized by both aerobic interval and continuous training protocols (Table S1). These data demonstrate that aerobic interval training improves running capacity and prolongs survival in tumor-bearing rats.

3.3. Exercise training restores redox homeostasis and improves muscle function in tumor-bearing rats

To determine the effects of exercise training on the skeletal muscle of tumor-bearing rats, we designed new experiments involving only aerobic interval training because our data indicated similar effects on running capacity between aerobic interval and continuous training protocols. We observed reduced activity of citrate synthase in the *plantaris* muscle from tumor-bearing rats, while exercise training partially reestablished citrate synthase activity toward control levels (Figure 2C). Furthermore, *plantaris* muscle from tumor-bearing rats had changes in several makers of oxidative stress, including reduced levels of total glutathione (Figure 2D) and GSH:GSSG ratio (Figure 2E), as well as increased levels of 4-hydroxyalkenals (HAE) (Figure S2C), malondialdehyde (MDA) (Figure S2D), and protein carbonyl levels (Figure 2F). MDA and HAE are indicators of lipid peroxidation and protein carbonylation is an irreversible oxidation reaction and a biomarker of oxidative damage [38,39]. Exercise training did not change MDA and HAE levels (Figures S2C–D), however, it did remarkably increase glutathione levels (Figure 2D–E) and decrease protein carbonylation (Figure 2F). There were no significant changes

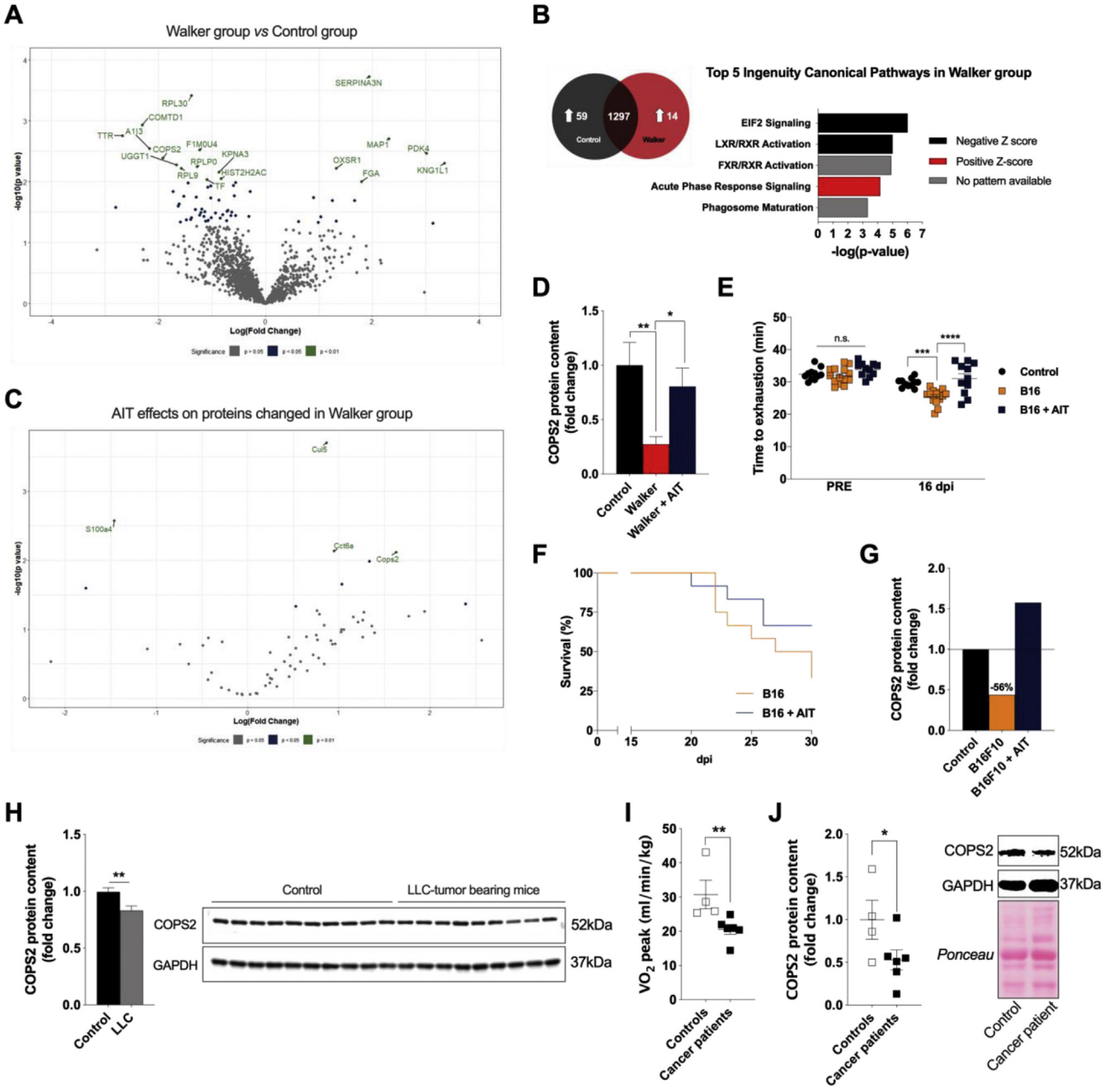

Figure 3: Effects of aerobic interval training (AIT) on muscle proteome in tumor-bearing rats and mice. (**A**) Volcano plot comparing the profile of the *plantaris* proteomes of control and tumor-bearing rats. $n = 5$ rats. (**B**) Number of proteins differentially expressed in the *plantaris* muscle from tumor-bearing rats. Overlap indicates proteins were not changed between groups Pathway enrichment analysis using upregulated and downregulated proteins. $n = 5$ rats. (**C**) Volcano plot showing the effects of AIT specifically in proteins changed in tumor-bearing rats. $n = 5$ rats. (**D**) COPS2 protein content in the *plantaris* muscle. $n = 5$ rats. (**E**) Running capacity and (**F**) survival rate in B16 tumor-bearing mice submitted or not to AIT. $n = 11-14$. (**G**) COPS2 protein content in the *plantaris* muscle in B16 tumor-bearing mice submitted or not to AIT. $n =$ pool of 8 mice for each group. (**H**) COPS2 protein content in the *plantaris* muscle in LLC tumor-bearing mice. $n = 9-10$ mice. (**I**) VO_2 peak from patients with NSCLC prior to first line therapy. $n = 4-6$ subjects. (**J**) Quantification and representative immunoblot for COPS2 protein content in the *vastus lateralis* muscle from patients with NSCLC. $n = 4-6$ subjects. Data are presented as mean $\pm$ s.e.m. $^{*}P < 0.05$; $^{**}P < 0.01$; $^{***}P < 0.001$; $^{****}P < 0.001$; n.s. not significant. dpi: days post injection.

for catalase activity (Figure S2E) or fluorescent DHE oxidation products (Figure S2F) among the experimental groups. Finally, we evaluated the proteasome activity in the *plantaris* muscle because the ubiquitin-proteasome proteolytic system is responsible for the removal of damaged proteins and plays a major role in protein quality control [16,40]. Interestingly, aerobic interval training increased proteasomal activity by ~2-fold (Figure 2G).

We analyzed skeletal muscle mass from tumor-bearing rats at early (11 dpi) and late (18 dpi) stages of cancer cachexia. Analyses at 18 dpi were restricted to about half of the initial cohort that survived until this stage. We did not find significant differences among all experimental groups in the skeletal muscle mass at 11 dpi (Figure 2H and Figure S2G). Tumor-bearing rats had muscle atrophy in glycolytic muscles at 18dpi (Figure 2H), with no significant differences in *soleus*

muscle (Figure S2G). Remarkably, exercise training attenuated muscle mass atrophy (Figure 2H) and fully restored the muscle contractile function to the control levels (Figure 2I and Fig. S2H). Collectively, these data indicate that exercise training reduces protein carbonyl levels, normalizes GSH:GSSG ratio, and increases proteasomal activity in the *plantaris* muscle of tumor-bearing rats, likely contributing to restoration of redox homeostasis and protein quality control. Additionally, exercise training attenuates muscle atrophy and improves skeletal muscle contractile function in tumor-bearing rats.

3.4. Aerobic interval training reverses changes in the skeletal muscle proteomic profile in tumor-bearing rats

To explore the mechanisms underlying the benefits induced by exercise training during cachexia progression, we performed an unbiased gel-free mass-spectrometry-based proteomic analysis in the serum and *plantaris* muscle from 1) healthy control rats, 2) tumor-bearing rats, and 3) tumor-bearing rats submitted to the aerobic interval training protocol. Because our aim was to identify changes that occurred prior to onset of muscle atrophy, we used samples collected at 11 dpi.

Exercise training did not change the expression of proteins affected in the serum of tumor-bearing rats (Figures S3A–C) which led us to speculate that the main effects of exercise training would occur directly in the skeletal muscle tissue. In this content, *plantaris* proteomics identified a total of 1370 proteins across all experimental groups, with 59 proteins significantly downregulated and 14 proteins significantly upregulated in the tumor-bearing rats (Figure 3A–B and Table S3). Ingenuity Pathway Analysis using differently expressed proteins revealed Eukaryotic Initiation Factor 2 (EIF2) signaling, liver X receptor/retinoid X receptor (LXR/RXR) activation, farnesoid X receptor/retinoid X receptor (FXR/RXR) activation, and acute phase response signaling as the most significantly affected pathways in tumor-bearing rats (Figure 3B). We next verified the effects of exercise training on the 73 proteins regulated in the *plantaris* muscle from tumor-bearing rats (Figure 3C). Exercise training significantly normalized the expression of 9 proteins and did not significantly increase or decrease any protein to the same direction of the cancer effects (Figure 3C). As a particularly interesting protein for further investigation, COPS2 was one of the most downregulated proteins in tumor-bearing rats and its expression was fully restored by exercise training as demonstrated by mass spectrometry (Figure 3D) and immunoblot (Figure S4A) analysis. Basically, COPS2 mRNA levels were not changed in tumor-bearing rats (Figure S4B), suggesting that reduced COPS2 protein content is a consequence of posttranslational modifications.

We simultaneously we performed an experiment to test whether exercise training would affect COPS2 protein content in healthy control rats. Exercise training increased glutathione levels in *plantaris* muscle of healthy rats (Figure S5) without additional effects in carbonyl levels, catalase activity, 26 S proteasome activity, and muscle mass (Figures S5A–E), suggesting that the beneficial effects of exercise training are greater in rats under catabolism conditions than in healthy rats. Likewise, exercise training did not change COPS2 protein content in healthy rats (Figure S5F).

To investigate whether the effects of cancer cachexia on COPS2 expression were also recapitulated in another cancer model with exercise intolerance, we investigated sedentary and trained B16F10 tumor-bearing mice. Consistent with data from the Walker 256 rat model, exercise training improved running capacity (Figure 3E) and tended to prolong survival in B16F10 tumor-bearing mice (Figure 3F) without affecting tumor progression (Figures S6A–B). B16F10 tumor-bearing mice had reduced running capacity but did not show significant body and muscle wasting by 16 dpi (Figures S6C–D). At this same timepoint, mass spectrometry and immunoblot analysis demonstrated decreased COPS2 protein content in the *plantaris* muscle from B16F10 tumor-bearing mice, which was fully normalized by exercise training (Figure 3G and Figure S5E). These findings corroborate data from the Walker rat model, showing that exercise training improves running capacity and reverses cancer-induced decrease in muscle COPS2 protein expression.

3.5. Lewis lung carcinoma (LLC) tumor-bearing mice and lung cancer patients have reduced muscle COPS2 protein content

We previously demonstrated that exercise training attenuates tumor growth in Lewis lung carcinoma (LLC) tumor-bearing mice, resulting in obvious benefits as a result of reduced tumor growth, including improved muscle function and prolonged lifespan (Alves et al., 2018). We discovered that LLC tumor-bearing mice also present reduced levels of COPS2 protein content (Figure 3H). Moreover, to determine whether muscle COPS2 protein content is associated with exercise tolerance in humans, we evaluated six patients with non-small-cell lung cancer (NSCLC), and four age- and gender-matched control subjects (Table S4). The patients with NSCLC patients displayed lower VO_2peak (Figure 3I) than the control subjects. A *vastus lateralis* muscle biopsy was performed in the patients with NSCLC and control subjects under resting conditions. Immunoblot analysis revealed lower muscle COPS2 protein content in patients with NSCLC compared with age-matched controls (Figure 3J). Thus, these findings demonstrate that patients with NSCLC who have impaired aerobic capacity have decreased muscle COPS2 protein content as observed in the rodent models.

3.6. Effects of COPS2 knockdown in primary human myotubes

To investigate the molecular pathways regulated by COPS2 in myotubes, we used a specific siRNA to knockdown COPS2 in primary human myotubes (Figure 4A,B). COPS2 knockdown did not change total protein content (Figure 4C), suggesting that COPS2 knockdown does not induce substantial cell death or atrophy. Microarray analysis using 3 independent experiments, and a cutoff at $p < 0.05$, exhibited 872 genes differently expressed after COPS2 knockdown (Figure 4D). Functional enrichment analysis in the context of the Kyoto Encyclopedia of Genes and Genomes (KEGG) databases demonstrated cellular pathways affected by COPS2 knockdown, including multiple pathways related to the regulation of actin cytoskeleton (Figure 4E). As demonstrated in a volcano plot (Figure 4F) and validated using RT-qPCR (Figure 4G), the two most downregulated genes were Alkylglycerone Phosphate Synthase (*AGPS*) and Cytoskeleton Associated Protein 4 (*CKAP*), while the two most upregulated genes were Chemerin Chemokine-Like Receptor 1 (*CMKLR1*) and Solute Carrier Family 7 Member 5 (*SLC7A5*). Among other important functions for cellular homeostasis of these genes, an interesting observation includes the upregulation of SLC7A5 mRNA levels, which codes a membrane transporter to uptake large amino acids [41] that can also mediate the transport of thyroid hormones translocation across the cell membrane [42,43]. Because COPS2 was previously shown to act as a corepressor of thyroid hormones activity, we speculate that this increase in *SLC7A5* mRNA levels could be an intrinsic compensatory cellular mechanism leading to increased thyroid hormone activity after COPS2 knockdown. Finally, we assessed whether these pathways could be associated with metabolic changes in myotubes with COPS2 knockdown using extracellular flux analysis. Interestingly, COPS2

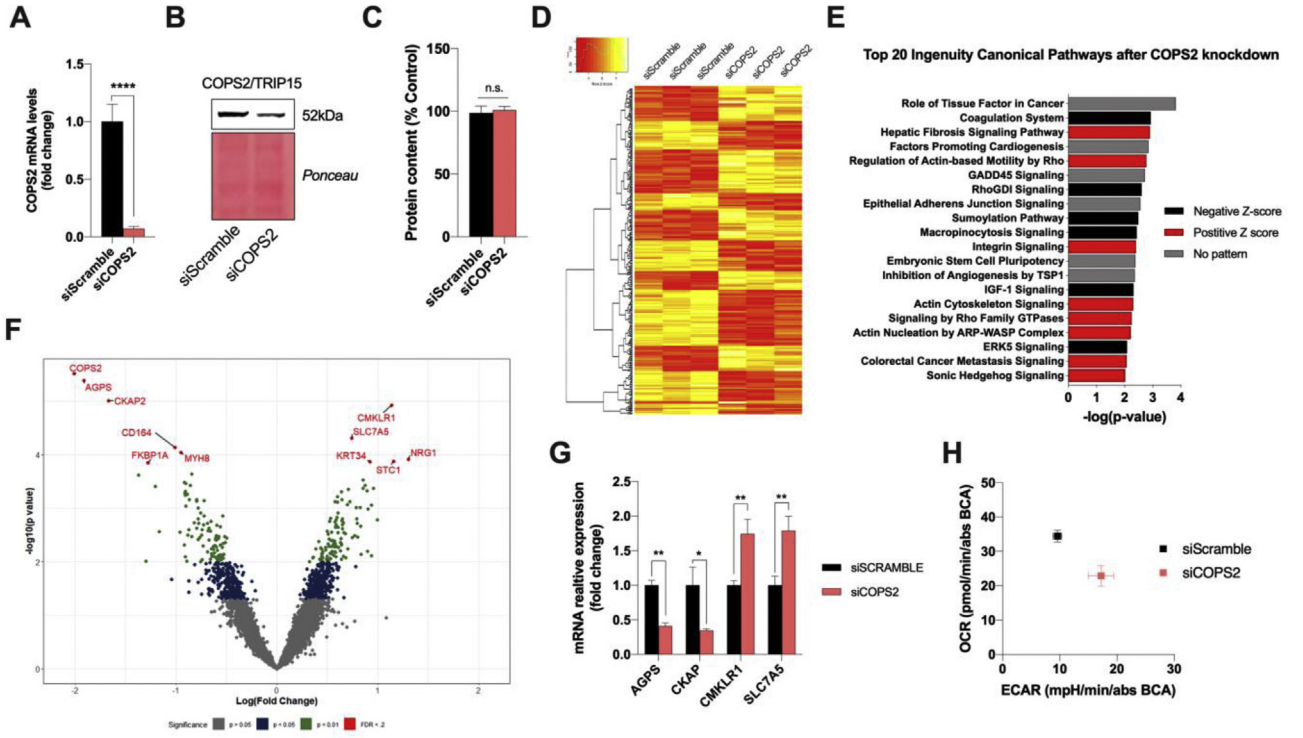

Figure 4: Effects of COPS2 knockdown in primary human myotubes. (**A**) COPS2 mRNA expression 48 h after transfection with a specific siRNA for COPS2. $n = 3$ independent experiments. (**B**) Immunoblot demonstrating efficiency of COPS2 knockdown. (**C**) Total protein content 48 h after COPS2 knockdown. $n = 3$ independent experiments. (**D**) Heatmap including genes differentially regulated by COPS2 knockdown. $n = 3$ independent experiments. (**E**) Most significant pathways affected by COPS2 knockdown. (**F**) Volcano plot with highlights for the genes most differentially regulated by COPS2 knockdown. $n = 3$ independent experiments. (G) RT-qPCR validation for the 4 genes most regulated by COPS2 knockdown. $n = 3$ independent experiments. (**H**) Energy map showing changes in oxygen consumption rate (OCR) and extracellular acidification rate (ECAR) after COPS2 knockdown. $n = 11$ technical replications. Data are presented as mean ± s.e.m. $^{*}P < 0.05$; $^{**}P < 0.01$; $^{****}P < 0.001$; n.s. not significant.

knockdown decreased basal oxygen consumption rate (OCR) and increased basal extracellular acidification rate (ECAR) (Figure 4H), indicating a basal metabolic switch in human myotubes. Thus, these experiments indicate that COPS2 knockdown can affect muscle cell homeostasis, including changes in pathways involved in the regulation of actin cytoskeleton.

3.7. LLC-conditioned media decreases COPS2 protein content in primary mouse myoblast-derived myotubes

To test whether factors produced by tumor cells could directly affect muscle COPS2 protein content, we established an *in vitro* model by challenging primary mouse myoblast-derived myotubes with tumor cell-conditioned media (Figure 5A). Myotubes incubated with B16 or LLC-conditioned media had progressive loss of protein content (Figure 5B,C). HeLa cell-conditioned medium was used as an additional control group and did not affect the myotube total protein content. We decided to use the LLC cell line for the following experiments because the effects of LLC-conditioned media were more pronounced than B16-conditioned media (Figure 5B–D). Notably, incubation with LLC-conditioned media significantly decreased COPS2 protein content in the myotubes (Figure 4E). Thus, these findings demonstrate that LLC cells produce factors that directly affect myotubes reducing COPS2 protein expression.

To test whether COPS2 overexpression or COPS2 knockdown could protect myotubes from LLC-induced catabolism, we first used an adenovirus vector to overexpress full length COPS2 protein in differentiated mouse myotubes (Figure 5F,G). COPS2 overexpression did not attenuate loss of protein levels (Figure 5H,I) or enhance metabolic demand and glutathione levels (Figs. S7A and B) induced by LLC-conditioned media in myotubes. Conversely, COPS2 knockdown (Figure S7C) significantly reduced the loss of protein levels (Figure 5J) and exacerbated glutathione levels induced by LLC-conditioned media (Figure 5K), suggesting that a decrease in muscle COPS2 protein expression could be a compensatory mechanism to attenuate cancer effects. This occurred with no significant changes in OCR or ECAR in mouse myotubes (Figure S7D). Neither COPS2 knockdown nor LLC-conditioned media affected MitoTracker signal in mouse myotubes (Figures S7E and F).

Because our microarray analysis has demonstrated that COPS2 knockdown affects multiple pathways that could regulate actin cytoskeleton, we next studied whether COPS2 knockdown and/or LLC-conditioned media would affect polymeric actin filament (F-actin) expression in mouse myotubes. Interestingly, incubation of mouse myotubes with LLC-conditioned media decreased F-actin expression, while COPS2 knockdown increased F-actin in both control myotubes and myotubes incubated with LLC-conditioned media (Figures 5L and M). Moreover, LLC-conditioned media increased 26 proteasome activity and decreased the Slc7a5 mRNA expression (Figure 5O), and these effects were attenuated by COPS2 knockdown (Figure 5N and O). Therefore, these data demonstrated that incubation with LLC-conditioned media decreases COPS2 protein content in myotubes, while COPS2 knockdown seems to compensate most of the LLC-conditioned media-induced effects in myotubes, suggesting that decreased COPS2 protein levels could be an intrinsic compensatory mechanism to protect myotubes from the effects of cancer.

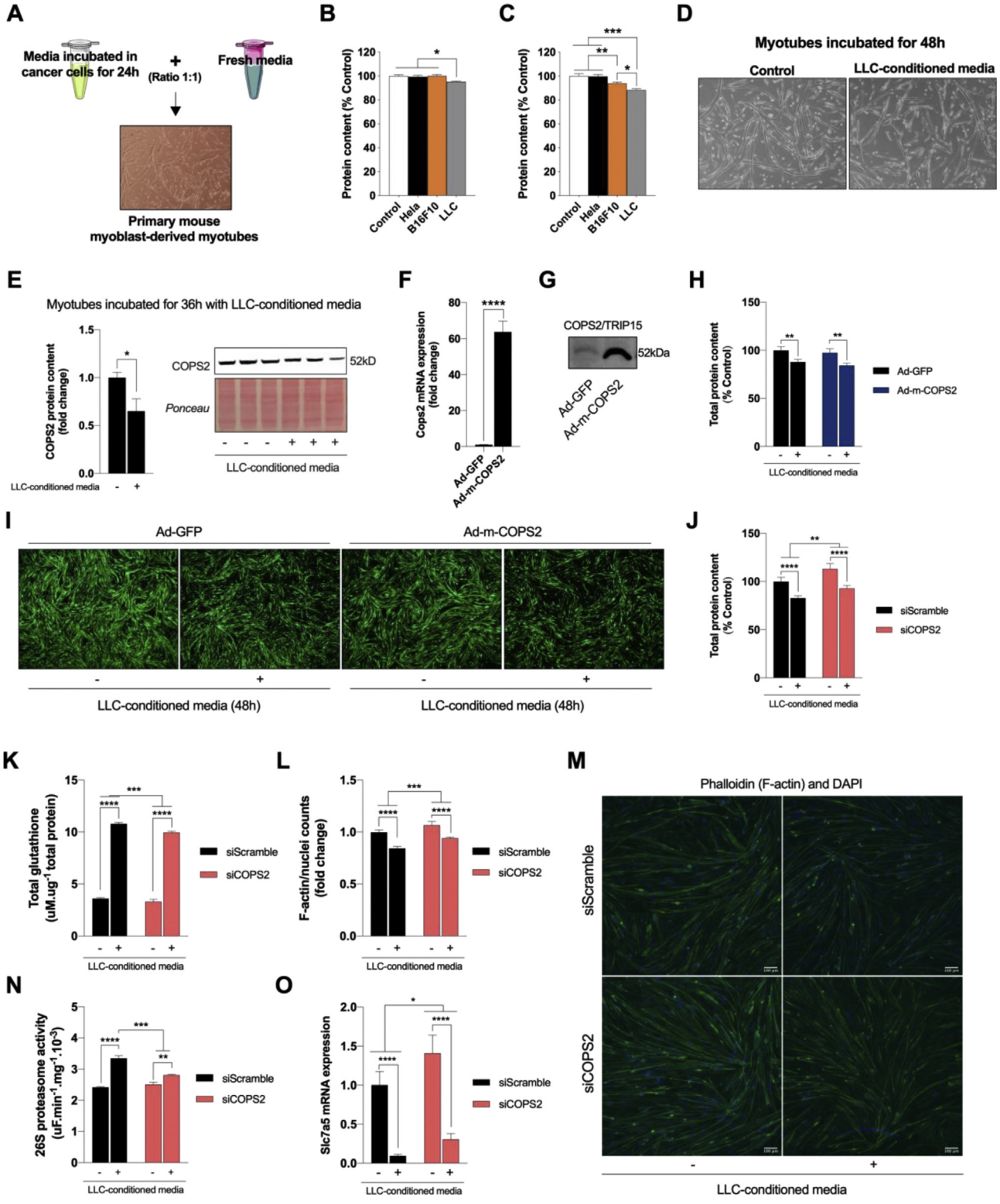

Figure 5: Effects of cancer-conditioned media in primary mouse myoblast-derived myotubes. (**A**) Experimental design to challenge myotubes with cancer-conditioned media. (**B** and **C**) Total protein content in myotubes treated for (**B**) 24 or (**C**) 48 h with media conditioned in HeLa, B16F10 or LLC tumor cells. $n = 3$ independent experiments. (**D**) Representative images of myotubes treated for 48 h with LLC-conditioned media. (**E**) COPS2 protein expression in myotubes treated with LLC conditioned media. $n = 3$ independent experiments. (**F**) Cops2 mRNA expression 48 h after transduction with an adenovirus vector-COPS2. $n = 3$ technical replications. (**G**) Immunoblot demonstrating efficiency of COPS2 overexpression. (**H** and **I**) Total protein content and representative images of myotubes with COPS2 overexpression with or without treatment with LLC-conditioned media for 48 h $n = 3–4$ technical replications. (**J**) Total protein content of myotubes with COPS2 knockdown with or without treatment with LLC-conditioned media for 48 h $n = 12$ technical replications. (**K**) Total glutathione. $n = 5$ technical replications. (**L** and **M**) F-actin expression. $n = 3–5$ technical replications. (**N**) 26 S proteasome activity. $n = 3$ technical replications. (**O**) Slc7a5 mRNA expression. $n = 6$ technical replications. Data are presented as mean ± s.e.m. $^{*}P < 0.05$, $^{**}P < 0.01$, $^{***}P < 0.001$, $^{****}P < 0.0001$. n.s. not significant.

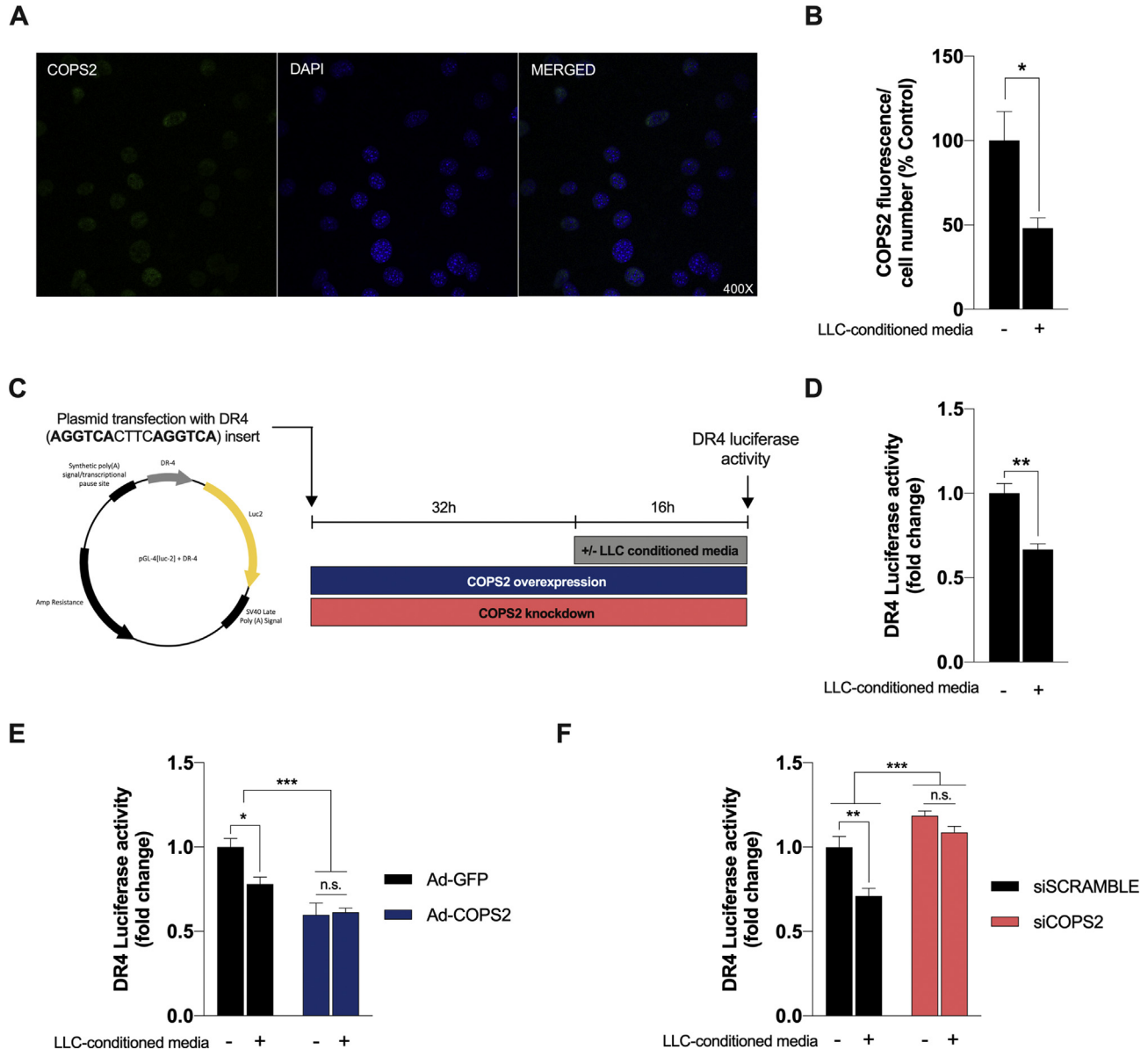

Figure 6: Effects of LLC-conditioned media and COPS2 regulation on a specific direct repeat 4 (DR4) response element activity. **(A)** Immunofluorescence demonstrating specific nuclear staining for COPS2 using a specific C-terminal antibody in C2C12 myoblasts. (**B**) Quantification of nuclear COPS2 expression with or without treatment with LLC-conditioned media in C2C12 myoblasts for 16 h $n = 6$ independent experiments. (**C**) Experimental design to analyze the effects of LLC-conditioned media and COPS2 regulation on DR4 activity using a luciferase reporter assay. (**D**) DR4 activity after LLC-conditioned media treatment. $n = 3$ independent experiments. (**E** and **F**) DR4 activity after COPS2 (**E**) overexpression or (**F**) knockdown with or without cancer-conditioned media treatment. $n = 3$ independent experiments. Data are presented as mean ± s.e.m. $^{*}P < 0.05$, $^{**}P < 0.01$, $^{***}P < 0.001$, $^{****}P < 0.0001$. n.s. not significant.

3.8. COPS2 regulates direct repeat 4 (DR4) response element activity in myotubes incubated with LLC-conditioned media

COPS2 is a key component of the COP9 signalosome complex, which regulates the Cullin-RING E3 ubiquitin ligases [44–46]. However, COPS2 also acts as a transcriptional corepressor by interacting with nuclear hormone receptors and this cellular function is independent of the COP9 signalosome complex [47–49]. Based on this cellular function, we hypothesized that LLC-conditioned media would affect the activity of nuclear hormone receptors and COPS2 would regulate this process through transcriptional corepressor activity. We therefore performed a series of experiments using C2C12 immortalized mouse myoblast cell line to test this hypothesis.

We first evaluated whether incubation with LLC-conditioned media affects nuclear COPS2 protein expression in these myoblasts. The C-terminal of COPS2 protein interacts with the other subunits of the assembled COP9 signalosome complex, while the N-terminal does not present protein-protein interactions [45]. Primary antibodies previously used in this study target the COPS2 N-terminal and, therefore, stains overall cellular COPS2 protein expression (Figure S8A and B). On the other hand, a specific antibody that targets only the COPS2 C-terminal (Abcam; Cat# ab155774) specifically stains the nuclear COPS2

expression in immunofluorescence experiments (Figure 6A). Using this specific C-terminal antibody, we found that incubation of myoblasts with LLC-conditioned media for 16 h decreased nuclear COPS2 protein expression by ~50% (Figure 6B).

Nuclear hormone receptors bind to hormone response elements in the DNA and regulate the gene expression in response to sensing molecules, including thyroid hormones [50]. One of the most characterized thyroid hormone response elements is the direct repeat 4 (DR4), which is composed of two half-sites, such as the AGGTCA hexamer, interposed with 4 base pairs (*e.g.* AGGTCACTTCAGGTCA) [50,51]. We inserted a sequence with 2 of this DR4 response element in a luciferase-containing plasmid (Figure S8C) and transfected into C2C12 myoblasts to further test the effects COPS2 overexpression or COPS2 knockdown with or without LLC-conditioned media incubation on DR4 luciferase activity (Figure 6C). LLC-conditioned media consistently decreased DR4 luciferase activity (Figure 6D). COPS2 overexpression also decreased DR4 luciferase activity without additional effects of LLC-conditioned media incubation (Figure 6E). Notably, COPS2 knockdown not only increased DR4 luciferase activity, but also inhibited the effects of LLC-conditioned media incubation (Figure 6F). These experiments emphasize the role of COPS2 as a transcriptional corepressor and, most importantly, demonstrate that COPS2 is required to decrease DR4 activity in myoblasts incubated with cancer-conditioned media.

4. DISCUSSION

It is expected that more than 60% of patients with advanced stages of cancer will develop cachexia [52]. Given the fast and devastating progression of cancer cachexia, identifying therapies to target skeletal muscle and improve oxidative metabolism at early stages of cachexia is a major research challenge. In the current study, we establish that exercise training counteracts cancer-induced oxidative stress and muscle wasting. While the mechanisms underlying cachexia are still not fully understood, for the first time our findings demonstrate that muscle COPS2 is one of the most downregulated proteins at the early stage of cachexia progression and exercise training can normalize muscle COPS2 to the control levels.

Previous studies have demonstrated that high-intensity AIT promotes superior outcomes for cardiac patients [53] and in a rat model of infarction [54]. For example, an AIT protocol consisting of four bouts at 90% of maximal heart rate for 4 min, with intervals of 3 min at 70% of maximal heart rate, was superior to ACT protocol (70% of maximal heart rate) in reducing the blood glucose level, improving endothelial function and enhancing muscle biogenesis in metabolic syndrome patients [55]. Therefore, in addition to traditional aerobic continuous training, we tested the effects of an aerobic interval training in this study. Our findings showed similar benefits on running capacity and lifespan after aerobic continuous training and aerobic interval training protocols in tumor-bearing rats. Thus, to simplify our study design in the next steps, we performed experiments with only aerobic interval training. With regard to the cancer cachexia models, we first tested the effects of exercise training in a severe cancer rat model with homogeneous tumor growth and mortality rate. To investigate whether the effects of exercise training would be recapitulated in another cancer model with exercise intolerance, we investigated sedentary and trained B16F10 tumor-bearing mice. Finally, we also provide data from the LLC tumor-bearing mice, in which we previously demonstrated that exercise training promotes important benefits [31]. By using various models of cancer cachexia, this study extended conclusions from previous contributions and provides novel pre-clinical evidence that exercise training may be a beneficial co-therapy for cancer cachexia. One limitation of this study is that at this point we cannot extend any of our findings to models or patients undergoing chemotherapy or other treatments.

A major finding of the current study is that exercise training prolonged the lifespan of tumor-bearing rats. We found that neither aerobic interval training nor aerobic continuous training could attenuate tumor progression in the Walker 256 (bone marrow) model, suggesting that improved survival was not due to a slower tumor growth rate. Respiratory failure is the main cause of death in cachectic cancer patients, and the most likely cause of death in the Walker 256 model [56,57]. Both aerobic interval and continuous training protocols reduced lung edema in tumor-bearing rats. We thus speculate that reduced lung edema and secondary improvements of respiratory function are the major causes in the underlying prolonged lifespan in the tumor-bearing rats subjected to aerobic interval or continuous training protocols. While we focused on the effects of exercise training in the *plantaris* muscle in this study, future studies will be important to explore the diaphragm muscle function because it may explain the therapeutic effects of exercise on lung function. Additionally, skeletal muscle is a tissue profoundly affected by cancer but rarely inhabited by metastatic cancer cells [58], and future studies are necessary to investigate the systemic effects of exercise training, including site-specific metastasis formation. Overall, the current findings suggest that exercise training is a potential adjuvant therapy for cancer patients. We advocate for the application of exercise protocols at early-stage development of cachexia and reinforce the importance of exercise protocols in the multimodal treatment for cancer cachexia [59].

Exercise training can increase the mobilization of immune cells to effectively target tumor cells and several studies have demonstrated beneficial effects of exercise training in de-escalating tumor growth in various animal models. Although the precise molecular mechanism of the underlying exercise training effects is not fully characterized, a previous study demonstrated that natural killer cell infiltration was significantly increased in B16 tumors from trained mice, and this effect was mediated by IL-6 signaling [30]. Another exercise-induced effect is increased local vessel perfusion, which could facilitate the action of immune cells to suppress tumor growth [60]. Among many other factors that could explain why not all exercise training protocols attenuate tumor progression in cancer models, we speculate that the main reason in our study was the rapid and severe progression of cancer in our model. The time-course of cancer progression in this model is most likely quicker than the adaptation induced by exercise training. In this context, most of the previous studies demonstrated benefits with exercise training beginning prior to tumor cell injection, and we consider that exercise training has limited effects when the protocol begins after tumor cell injection because it requires time to induce the appropriate adaptation. Other factors that could explain the various findings include the different cancer types and the location of cancer cell injection, as well as the high variability observed in some models such as in our B16 tumor-bearing mice. Finally, identifying the best exercise training protocol to activate immune cells is a necessary step in future studies.

Another striking finding of the current study is that exercise training improved the redox homeostasis in the skeletal muscle of tumor-bearing rats. Over the past years, our group has been studying the therapeutic effects of exercise training for cardiac cachexia. These studies demonstrated that cardiomyopathy is associated with systemic inflammation and exacerbated oxidative stress, leading to skeletal muscle atrophy and weakness, and that exercise training re-established the redox homeostasis and protein quality control toward

control levels [16—18,54,61]. For the first time we report that aerobic interval training improves redox homeostasis and attenuates muscle contractile dysfunction in tumor-bearing rats that survived more than two weeks. Of note, exercise training increased proteasome activity, which we understand to be an adaptation to remove oxidized proteins and maintain quality control, allowing novel protein synthesis. Furthermore, soleus muscle was the only assessed muscle that did not undergo atrophy in tumor-bearing rats. *Soleus* has a predominance of type I fibers and previous studies demonstrated that type I fibers display higher oxidative capacity and lower response to cachexia [62]. This indicates that highly oxidative tissues have mechanisms to protect from the cachectic factors and this protection of oxidative muscle fibers has been attributed, at least in part, to the antioxidant capacity [63—65].

Animal models have been useful in determining numerous mechanisms behind muscle wasting. However, animal models have important limitations and caution is necessary to translate those findings to patients. For example, a recent study reported that two of the most common xenograft mouse cachexia models do not recapitulate changes in gene expression of cachectic pancreatic ductal adenocarcinoma patients, a cancer type with a high prevalence of cachexia [66]. For instance, *Atg5* and *Bnip3* mRNA expression, two genes related to autophagy process, were not changed in pancreatic ductal adenocarcinoma patients, but increased in skeletal muscle from both C26 and LLC mice [66]. Importantly, other models such as orthotopic models or patient-derived xenograft exhibit improvements over classic xenograft models, but also present challenges in replicating human cancer cachexia. Finally, while tumor size usually represents less than 1% of body mass in humans, the tumor grows too fast and reaches more than 10% of the host body mass in most animal models. We have validated some of our findings in patients with lung cancer, showing that these patients have impaired aerobic capacity and decreased muscle COPS2 protein content as observed in the rodent models. In future studies, we will need to characterize other large cohorts, including other types of cancer and patients under treatment.

We sought to determine the molecular mechanisms associated with muscle wasting in our model. To understand the implications of the proteins altered in the mass spectrometry analysis, we used pathway analysis to define the canonical cellular pathways affected at the early stage of cancer cachexia. We found that acute phase response signaling was one of the most upregulated pathways in the serum of tumor-bearing rats. This was not surprising, because the acute phase response is the innate systemic early-defense activated by neoplasia and inflammation [67]. Two other affected pathways in the tumor-bearing rats were LXR/RXR activation and FXR/RXR activation. LXR/RXR and FXR/RXR heterodimers are members of the nuclear receptor superfamily and key players in the control of metabolic pathways, including lipid and glucose metabolism [68—71]. RXR heterodimers act as ligand-dependent transcriptional regulators and increase the DNA-binding efficiency of their partners, including not only LXR or FXR, but also the peroxisome proliferator-activated receptor α (PPARα), retinoic acid receptor (RAR), vitamin D receptor (VDR), thyroid hormone receptor (TR), and others [68—71]. Thus, future investigations should focus on the precise upstream mechanisms that regulate the activation or inhibition of RXR heterodimers during cancer cachexia progression.

Muscle COPS2 was one of the most downregulated proteins in tumor-bearing rats and mice and aerobic interval training normalized the muscle COPS2 protein content. COPS2 is expressed in most tissues (gtexportal.org/home), acts as a transcriptional corepressor by interacting with nuclear hormone receptors [47—49], and it is also a component of the COP9 signalosome complex that is responsible for deneddylation of Cullin-RING E3 ubiquitin ligases [44—46]. A recent study reported that only COPS2, but not other members of the COPS signalosome complex, is implicated in pluripotency maintenance of human embryonic stem cells [72]. The role of COPS2 for skeletal muscle homeostasis has not been previously determined. Because we did not observe changes in other subunits of the COP9 signalosome complex in tumor-bearing rats using mass spectrometry analysis, we suggest that decreased COPS2 protein content is more likely a result of changes in its corepressor role during the development of cancer cachexia. Interestingly, in our experiments COPS2 knockdown not only increased the DR4 response element activity, but also inhibited the effects of LLC-conditioned media in this DR4 activity, suggesting that COPS2 acts as a transcriptional corepressor and is required to mediate the effects of cancer-conditioned media incubation. Additionally, it is well established that binding of agonist ligands to RXR would result in dissociation of corepressors [48,68—71]. Based on this collective evidence, we speculate that COPS2 is dissociated and is degraded as a compensatory mechanism to protect myotubes from the cachexia-induced factors under muscle-wasting conditions. However, because exercise training attenuates the oxidative stress and other potential stressors, this compensatory mechanism would not be activated. Finally, COPS2 knockdown affected multiple pathways that could regulate actin cytoskeleton and COPS2 knockdown increased F-actin expression in myotubes. The actin cytoskeleton is a collection of actin filaments and regulatory proteins that regulate cell contractility [73,74]. Indeed, the actin cytoskeleton is the primary force-generating machinery in the cell and while the mechanisms linking COPS2 cellular function to the regulation of actin cytoskeleton are unknown, we speculate that decreases in COPS2 could also be a compensatory process to attenuate the loss of contractile capacity in skeletal muscle. Future research will be necessary to understand these protein-protein interactions in the context of oxidative stress.

Our findings demonstrate that LLC cells produce factors that directly affect myotubes reducing COPS2 protein expression. Identifying factors produced by tumors or other tissues in response to tumor progression that could induce muscle atrophy is of major scientific interest. Recent discoveries have uncovered some of these catabolic mediators, including fatty acids [75], microvesicles [76], TGF-β [77], parathyroid hormone-related protein [78], Ataxin-10 [79] and multiple pro-inflammatory cytokines [14]. Upcoming studies investigating these factors in the context of DR4 response element activity in myoblasts/myotubes will be highly relevant.

The current study has important clinical implications. Despite the variability commonly observed in human studies, we found reduced muscle COPS2 protein content in lung cancer patients compared with healthy controls. Cachexia is a negative prognostic in patients with NSCLC [80], and identifying simple biomarkers that could detect skeletal muscle impairment prior to observable changes in the body composition is critical in clinical settings. While a muscle biopsy is invasive and difficult to incorporate into clinical practice, potential circulating factors associated with LXR/RXR or FXR/RXR activation, including COPS2/TRIP15/ALIEN, are potential candidates for testing. This study focused on the role of COPS2 in the skeletal muscle. However, by mining other studies, we found that Yang et al. (2016) applied a proteomics approach in the serum of gastric cancer patients and healthy controls and COPS2 was the most significant differently expressed protein between cancer patients and controls, leading the authors to conclude that COPS2 constitutes a novel biomarker for gastric cancer diagnosis [81]. Based on these findings, we have

initiated a study to determine circulating COPS2 levels in a large cohort of patient with lung cancer (clinicaltrial.gov NCT03960034).
In summary, the current study raises the concept of exercise training as a co-therapy for cancer cachexia and uncovers muscle COPS2 as one of the most downregulated proteins in cancer cachexia conditions which is normalized by exercise training.

AUTHORS' CONTRIBUTIONS

CRRA and PCB conceived and designed the study. CRRA, WN, NRA, VAV, GCT, LRGB, CGC and DF carried out animal procedures. CRRA and PRJ conducted *in vitro* procedures and assays. LH, AS, and GS carried out MS analysis. CRRA, WN, EJE, PRJ, VAV, GCT, LRGB, CGC, DF, and PCB acquired data. WN, MJNNA, CEN, and GCJ performed human studies. CEN, GS, UW, MFH, GCJR, RC, KJS, JLR, LJG, and PCB provided laboratory support and supervised the experiments. CRRA and EJE performed data analysis. CRRA drafted the manuscript. All authors interpreted the data, participated in manuscript review, and approved the final manuscript.

ACKNOWLEDGMENT

C.R.R.A. was supported by FAPESP, São Paulo, Brazil (2016/01478-0, 2014/03016-8, 2012/25240-1 and 2012/02528-0). P.C.B. was supported by Conselho Nacional de Pesquisa e Desenvolvimento (CNPq 306261/2016-2) and FAPESP (Sprint 16/50336-3). W.N. was supported by FAPESP, São Paulo, Brazil (2016/20187-6). This work was supported in part by a grant from FAPESP (2015/22814-5). J.B.N.M was supported by grants from the Norwegian Health Association and the Research Council of Norway (#275714). C.E.N was supported by Conselho Nacional de Desenvolvimento Científico e Tecnológico (CNPq, 303573/2015-5). K.J.S was supported by NICHD R01HD054599, Biogen and Cure SMA. L.J.G. was supported by NIH grants R01DK099511 and R01DK101043 and the Joslin Diabetes Center DRC (P30 DK36836). MS analysis was provided by the Proteomics and Modomics Experimental Core Facility (PROMEC) funded by the Faculty of Medicine at the Norwegian University of Science and Technology (NTNU) and the Central Norway Regional Health Authority. Data storage and handling is supported under the Norwegian research data archival system (NIRD)/Notur project NN9036K. The mass spectrometry proteomics data have been deposited at the ProteomeXchange Consortium via the PRIDE partner repository with the dataset identifier PXD013226. We thank Antonio Oliveira, Salome Da Silva Duarte Lepez, Rafael Azevedo, Reid Garner, and Dr. Vanessa P. Gutierrez for helpful technical support.

CONFLICTS OF INTEREST

None declared.

APPENDIX A. SUPPLEMENTARY DATA

Supplementary data to this article can be found online at https://doi.org/10.1016/j.molmet.2020.101012.

REFERENCES

[1] Brown, J.L., Rosa-Caldwell, M.E., Lee, D.E., Blackwell, T.A., Brown, L.A., Perry, R.A., et al., 2017. Mitochondrial degeneration precedes the development of muscle atrophy in progression of cancer cachexia in tumour-bearing mice. Journal of Cachexia, Sarcopenia and Muscle. https://doi.org/10.1002/jcsm.12232.

[2] Blackwell, T.A., Cervenka, I., Khatri, B., Brown, J.L., Rosa-Caldwell, M.E., Lee, D.E., et al., 2018. A transcriptomic analysis of the development of skeletal muscle atrophy in cancer-cachexia in tumor-bearing mice. Physiological Genomics. https://doi.org/10.1152/physiolgenomics.00061.2018.

[3] Petruzzelli, M., Wagner, E.F., 2016. Mechanisms of metabolic dysfunction in cancer-associated cachexia. Genes & Development. https://doi.org/10.1101/gad.276733.115.

[4] Petruzzelli, M., Schweiger, M., Schreiber, R., Campos-Olivas, R., Tsoli, M., Allen, J., et al., 2014. A switch from white to Brown fat increases energy expenditure in cancer-associated cachexia. Cell Metabolism, 1–15. https://doi.org/10.1016/j.cmet.2014.06.011.

[5] Hardee, J.P., Montalvo, R.N., Carson, J.A., 2017. Linking cancer cachexia-induced anabolic resistance to skeletal muscle oxidative metabolism. Oxidative Medicine and Cellular Longevity. https://doi.org/10.1155/2017/8018197.

[6] Fearon, K.C.H., Glass, D.J., Guttridge, D.C., 2012. Cancer cachexia: mediators, signaling, and metabolic pathways. Cell Metabolism 16(2):153–166. https://doi.org/10.1016/j.cmet.2012.06.011.

[7] Constantinou, C., De Oliveira, C.C.F., Mintzopoulos, D., Busquets, S., He, J., Kesarwani, M., et al., 2011. Nuclear magnetic resonance in conjunction with functional genomics suggests mitochondrial dysfunction in a murine model of cancer cachexia. International Journal of Molecular Medicine 27(1):15–24. https://doi.org/10.3892/ijmm.2010.557.

[8] Aria Tzika, A., Fontes-Oliveira, C.C., Shestov, A.A., Constantinou, C., Psychogios, N., Righi, V., et al., 2013. Skeletal muscle mitochondrial uncoupling in a murine cancer cachexia model. International Journal of Oncology 43(3):886–894. https://doi.org/10.3892/ijo.2013.1998.

[9] Fermoselle, C., García-Arumí, E., Puig-Vilanova, E., Andreu, A.L., Urtreger, A.J., de Kier Joffé, E.D.B., et al., 2013. Mitochondrial dysfunction and therapeutic approaches in respiratory and limb muscles of cancer cachectic mice. Experimental Physiology 98(9):1349–1365. https://doi.org/10.1113/expphysiol.2013.072496.

[10] Collins, P., Bing, C., McCulloch, P., Williams, G., 2002. Muscle UCP-3 mRNA levels are elevated in weight loss associated with gastrointestinal adenocarcinoma in humans. British Journal of Cancer 86(3):372–375. https://doi.org/10.1038/sj.bjc.6600074.

[11] Der-Torossian, H., Wysong, A., Shadfar, S., Willis, M.S., McDunn, J., Couch, M.E., 2013. Metabolic derangements in the gastrocnemius and the effect of Compound A therapy in a murine model of cancer cachexia. Journal of Cachexia, Sarcopenia and Muscle 4(2):145–155. https://doi.org/10.1007/s13539-012-0101-7.

[12] Springer, J., Hartmann, A., Palus, S., Adams, V., Von Harsdorf, R., Anker, S.D., et al., 2009. The xanthine oxidase inhibitors oxypurinol and allopurinol reduce wasting and improve cardiac function in experimental cancer cachexia. Journal of Cardiac Failure 1:S22. https://doi.org/10.1016/j.cardfail.2009.06.381.

[13] Argilés, J.M., Busquets, S., Stemmler, B., López-Soriano, F.J., 2014. Cancer cachexia: understanding the molecular basis. Nature Reviews Cancer 14(11):754–762. https://doi.org/10.1038/nrc3829.

[14] Argilés, J.M., Stemmler, B., López-Soriano, F.J., Busquets, S., 2018. Inter-tissue communication in cancer cachexia. Nature Reviews Endocrinology. https://doi.org/10.1038/s41574-018-0123-0.

[15] Porporato, P.E., 2016. Understanding cachexia as a cancer metabolism syndrome. Oncogenesis. https://doi.org/10.1038/oncsis.2016.3.

[16] Alves, C.R.R., Da Cunha, T.F., Da Paixão, N.A., Brum, P.C., 2015. Aerobic exercise training as therapy for cardiac and cancer cachexia. Life Sciences, 9–14.

[17] Cunha, T.F., Bechara, L.R.G., Bacurau, A.V.N., Jannig, P.R., Voltarelli, V.A., Dourado, P.M., et al., 2017. Exercise training decreases NADPH oxidase activity and restores skeletal muscle mass in heart failure rats. Journal of Applied Physiology. https://doi.org/10.1152/japplphysiol.00182.2016.

[18] Cunha, T.F., Bacurau, A.V.N., Moreira, J.B.N., Paixão, N.A., Campos, J.C., Ferreira, J.C.B., et al., 2012. Exercise training prevents oxidative stress and ubiquitin-proteasome system overactivity and reverse skeletal muscle atrophy in heart failure. PloS One 7(8). https://doi.org/10.1371/journal.pone.0041701.

[19] Bechara, L.R.G., Moreira, J.B.N., Jannig, P.R., Voltarelli, V.A., Dourado, P.M., Vasconcelos, A.R., et al., 2014. NADPH oxidase hyperactivity induces plantaris atrophy in heart failure rats. International Journal of Cardiology 175(3):499–507. https://doi.org/10.1016/j.ijcard.2014.06.046.

[20] Egan, B., Zierath, J.R., 2013. Exercise metabolism and the molecular regulation of skeletal muscle adaptation. Cell Metabolism 17(2):162–184. https://doi.org/10.1016/j.cmet.2012.12.012.

[21] Alves, C.R.R., da Cunha, T.F., da Paixão, N.A., Brum, P.C., 2014. Aerobic exercise training (AET) as therapy for cardiac and cancer cachexia. Life Sciences. https://doi.org/10.1016/j.lfs.2014.11.029.

[22] Gielen, S., Laughlin, M.H., O'Conner, C., Duncker, D.J., 2015. Exercise training in patients with heart disease: review of beneficial effects and clinical recommendations. Progress in Cardiovascular Diseases 57(4):347–355. https://doi.org/10.1016/j.pcad.2014.10.001.

[23] Pedersen, B.K., Saltin, B., 2015. Exercise as medicine - evidence for prescribing exercise as therapy in 26 different chronic diseases. Scandinavian Journal of Medicine & Science in Sports 25:1–72. https://doi.org/10.1111/sms.12581.

[24] Nobre, T.S., Antunes-Correa, L.M., Groehs, R.V., Alves, M.N., Sarmento, A.O., Bacurau, A.V., et al., 2016. Exercise training improves neurovascular control and calcium cycling gene expression in heart failure patients with cardiac resynchronization therapy. American Journal of Physiology - Heart and Circulatory Physiology 5511. https://doi.org/10.1152/ajpheart.00275.2016 ajpheart 00275 2016.

[25] Benatti, F.B., Pedersen, B.K., 2014. Exercise as an anti-inflammatory therapy for rheumatic diseases—myokine regulation. Nature Reviews Rheumatology 11(2):86–97. https://doi.org/10.1038/nrrheum.2014.193.

[26] Hillman, C.H., Erickson, K.I., Kramer, A.F., 2008. Be smart, exercise your heart: exercise effects on brain and cognition. Nature Reviews Neuroscience 9(1):58–65. https://doi.org/10.1038/nrn2298.

[27] Jones, L.W., Eves, N.D., Scott, J., 2017. Bench-to-Bedside approaches for personalized exercise therapy in cancer. American Society of Clinical Oncology Education Book 37:684–694. https://doi.org/10.14694/EDBK_173836.

[28] Hayes, S.C., Newton, R.U., Spence, R.R., Galvão, D.A., 2019. The Exercise and Sports Science Australia position statement: exercise medicine in cancer management. Journal of Science and Medicine in Sport. https://doi.org/10.1016/j.jsams.2019.05.003.

[29] Campbell, K.L., Winters-Stone, K.M., Wiskemann, J., May, A.M., Schwartz, A.L., Courneya, K.S., et al., 2019. Exercise Guidelines for cancer survivors: consensus statement from international multidisciplinary roundtable. Medicine & Science in Sports & Exercise. https://doi.org/10.1249/MSS.0000000000002116.

[30] Pedersen, L., Idorn, M., Olofsson, G.H., Lauenborg, B., Nookaew, I., Hansen, R.H., et al., 2016. Voluntary running suppresses tumor growth through epinephrine- and IL-6-dependent NK cell mobilization and redistribution. Cell Metabolism 23(3):554–562. https://doi.org/10.1016/j.cmet.2016.01.011.

[31] Alves, C.R.R., das Neves, W., Tobias, G.C., Almeida, N.R., Barreto, R.F., Melo, C.M., et al., 2018. High-intensity interval training slows down tumor progression in mice bearing Lewis lung carcinoma. JCSM Rapid Communications 1(2):e00060.

[32] Bacurau, A.V.N., Belmonte, M.A., Navarro, F., Moraes, M.R., Pontes, F.L., Pesquero, J.L., et al., 2007. Effect of a high-intensity exercise training on the metabolism and function of macrophages and lymphocytes of Walker 256 tumor-bearing rats. Experimental Biology and Medicine 232(10):1289–1299. https://doi.org/10.3181/0704-RM-93.

[33] Penna, F., Busquets, S., Pin, F., Toledo, M., Baccino, F.M., López-Soriano, F.J., et al., 2011. Combined approach to counteract experimental cancer cachexia: eicosapentaenoic acid and training exercise. Journal of Cachexia, Sarcopenia and Muscle 2(2):95–104. https://doi.org/10.1007/s13539-011-0028-4.

[34] Lira, F.S., Tavares, F.L., Yamashita, A.S., Koyama, C.H., Alves, M.J., Caperuto, E.C., et al., 2008. Effect of endurance training upon lipid metabolism in the liver of cachectic tumour-bearing rats. Cell Biochemistry and Function 26(6):701–708. https://doi.org/10.1002/cbf.1495.

[35] Pin, F., Busquets, S., Toledo, M., Camperi, A., Lopez-Soriano, F.J., Costelli, P., et al., 2015. Combination of exercise training and erythropoietin prevents cancer-induced muscle alterations. Oncotarget 6(41):43202–43215. https://doi.org/10.18632/oncotarget.6439.

[36] Alves, C.R.R., Faria, D.D.P., Carneiro, C.D.G., Garcez, A.T., Gutierrez, V.P., das Neves, W., et al., 2018. ^{18}F-Fluoride PET/CT and ^{99m}Tc-MDP SPECT/CT can detect bone cancer at early stage in rodents. Life Sciences 206. https://doi.org/10.1016/j.lfs.2018.05.030.

[37] Medeiros, A., Rolim, N.P.L., Oliveira, R.S.F., Rosa, K.T., Mattos, K.C., Casarini, D.E., et al., 2008. Exercise training delays cardiac dysfunction and prevents calcium handling abnormalities in sympathetic hyperactivity-induced heart failure mice. Journal of Applied Physiology (Bethesda, Md. : 1985). https://doi.org/10.1152/japplphysiol.00493.2007.

[38] Souza, R.W.A., Alves, C.R.R., Medeiros, A., Rolim, N., Silva, G.J.J., Moreira, J.B.N., et al., 2018. Differential regulation of cysteine oxidative post-translational modifications in high and low aerobic capacity. Scientific Reports 8(1):17772. https://doi.org/10.1038/s41598-018-35728-2.

[39] Poole, L.B., Nelson, K.J., 2008. Discovering mechanisms of signaling-mediated cysteine oxidation. Current Opinion in Chemical Biology. https://doi.org/10.1016/j.cbpa.2008.01.021.

[40] Campos, J.C., Queliconi, B.B., Dourado, P.M.M., Cunha, T.F., Zambelli, V.O., Bechara, L.R.G., et al., 2012. Exercise training restores cardiac protein quality control in heart failure. PloS One 7(12). https://doi.org/10.1371/journal.pone.0052764.

[41] Mastroberardino, L., Spindler, B., Pfeiffer, R., Skelly, P.J., Loffing, J., Shoemaker, C.B., et al., 1998. Amino-acid transport by heterodimers of 4F2hc/CD98 and members of a permease family. Nature. https://doi.org/10.1038/26246.

[42] Friesema, E.C.H., Docter, R., Moerings, E.P.C.M., Verrey, F., Krenning, E.P., Hennemann, G., et al., 2001. Thyroid hormone transport by the heterodimeric human system L amino acid transporter. Endocrinology. https://doi.org/10.1210/endo.142.10.8418.

[43] Kim, D.K., Kanai, Y., Choi, H.W., Tangtrongsup, S., Chairoungdua, A., Babu, E., et al., 2002. Characterization of the system L amino acid transporter in T24 human bladder carcinoma cells. Biochimica et Biophysica Acta (BBA) - Biomembranes. https://doi.org/10.1016/S0005-2736(02)00516-3.

[44] Lykke-Andersen, K., Schaefer, L., Menon, S., Deng, X.-W., Miller, J.B., Wei, N., 2003. Disruption of the COP9 signalosome Csn2 subunit in mice causes deficient cell proliferation, accumulation of p53 and cyclin E, and early embryonic death. Molecular and Cellular Biology 23(19):6790–6797. https://doi.org/10.1128/MCB.23.19.6790–6797.2003.

[45] Lingaraju, G.M., Bunker, R.D., Cavadini, S., Hess, D., Hassiepen, U., Renatus, M., et al., 2014. Crystal structure of the human COP9 signalosome. Nature. https://doi.org/10.1038/nature13566.

[46] Cavadini, S., Fischer, E.S., Bunker, R.D., Potenza, A., Lingaraju, G.M., Goldie, K.N., et al., 2016. Cullin-RING ubiquitin E3 ligase regulation by the COP9 signalosome. Nature. https://doi.org/10.1038/nature17416.

[47] Moehren, U., Papaioannou, M., Reeb, C.A., Hong, W., Baniahmad, A., n.d. Alien interacts with the human androgen receptor and inhibits prostate cancer cell growth, Doi: 10.1210/me.2006-0468.

[48] Dressel, U., Thormeyer, D., Altincicek, B., Paululat, A., Eggert, M., Schneider, S., et al., 1999. Alien, a highly conserved protein with characteristics of a. Corepressor for Members of the Nuclear Hormone Receptor Superfamily 19(5):3383–3394.

[49] Papaioannou, M., Melle, C., Baniahmad, A., 2007. The coregulator Alien. Nuclear Receptor Signaling 5. https://doi.org/10.1621/nrs.05008.

[50] Paquette, M.A., Atlas, E., Wade, M.G., Yauk, C.L., 2014. Thyroid hormone response element half-site organization and its effect on thyroid hormone mediated transcription. PloS One. https://doi.org/10.1371/journal.pone.0101155.

[51] Apfel, R., Benbrook, D., Lernhardt, E., Ortiz, M.A., Salbert, G., Pfahl, M., 1994. A novel orphan receptor specific for a subset of thyroid hormone-responsive elements and its interaction with the retinoid/thyroid hormone receptor subfamily. Molecular and Cellular Biology. https://doi.org/10.1128/mcb.14.10.7025.

[52] von Haehling, S., Morley, J.E., Anker, S.D., 2010. An overview of sarcopenia: facts and numbers on prevalence and clinical impact. Journal of Cachexia, Sarcopenia and Muscle. https://doi.org/10.1007/s13539-010-0014-2.

[53] Wisloff, U., Stoylen, A., Loennechen, J.P., Bruvold, M., Rognmo, O., Haram, P.M., et al., 2007. Superior cardiovascular effect of aerobic interval training versus moderate continuous training in heart failure patients: a randomized study. Circulation 115(24):3086–3094. https://doi.org/10.1161/CIRCULATIONAHA.106.675041.

[54] Moreira, J.B.N., Bechara, L.R.G., Bozi, L.H.M., Jannig, P.R., Monteiro, A.W.a., Dourado, P.M., et al., 2013. High- versus moderate-intensity aerobic exercise training effects on skeletal muscle of infarcted rats. Journal of Applied Physiology (Bethesda, Md.: 1985) 114(8):1029–1041. https://doi.org/10.1152/japplphysiol.00760.2012.

[55] Tjønna, A.E., Lee, S.J., Rognmo, Ø., Stølen, T.O., Bye, A., Haram, P.M., et al., 2008. Aerobic interval training versus continuous moderate exercise as a treatment for the metabolic syndrome: a pilot study. Circulation 118(4):346–354. https://doi.org/10.1161/CIRCULATIONAHA.108.772822.

[56] Roberts, B.M., Ahn, B., Smuder, A.J., Al-Rajhi, M., Gill, L.C., Beharry, A.W., et al., 2013. Diaphragm and ventilatory dysfunction during cancer cachexia. Federation of American Societies for Experimental Biology Journal. https://doi.org/10.1096/fj.12-222844.

[57] Dhanapal, R., Saraswathi, T., Govind, R.N., 2011. Cancer cachexia. Journal of Oral and Maxillofacial Pathology 15(3):257–260. https://doi.org/10.4103/0973-029X.86670.

[58] Biswas, A.K., Acharyya, S., 2020. Understanding cachexia in the context of metastatic progression. Nature Reviews Cancer. https://doi.org/10.1038/s41568-020-0251-4.

[59] Solheim, T.S., Laird, B.J.A., Balstad, T.R., Bye, A., Stene, G., Baracos, V., et al., 2018. Cancer cachexia: rationale for the MENAC (multimodal - exercise, nutrition and anti-inflammatory medication for cachexia) trial. BMJ Supportive & Palliative Care. https://doi.org/10.1136/bmjspcare-2017-001440.

[60] Betof, A.S., Lascola, C.D., Weitzel, D., Landon, C., Scarbrough, P.M., Devi, G.R., et al., 2015. Modulation of murine breast tumor vascularity, hypoxia and chemotherapeutic response by exercise. Journal of the National Cancer Institute 107(5). https://doi.org/10.1093/jnci/djv040.

[61] Brum, P.C., Bacurau, A.V., Cunha, T.F., Bechara, L.R.G., Moreira, J.B.N., 2014. Skeletal myopathy in heart failure: effects of aerobic exercise training. Experimental Physiology 99(4):616–620. https://doi.org/10.1113/expphysiol.2013.076844.

[62] Acharyya, S., Butchbach, M.E.R., Sahenk, Z., Wang, H., Saji, M., Carathers, M., et al., 2005. Dystrophin glycoprotein complex dysfunction: a regulatory link between muscular dystrophy and cancer cachexia. Cancer Cell 8(5):421–432. https://doi.org/10.1016/j.ccr.2005.10.004.

[63] Jannig, P.R., Alves, C.R.R., Voltarelli, V.A., Bozi, L.H.M., Vieira, J.S., Brum, P.C., et al., 2017. Effects of N-acetylcysteine on isolated skeletal muscle contractile properties after an acute bout of aerobic exercise. Life Sciences. https://doi.org/10.1016/j.lfs.2017.10.012.

[64] Li, P., Waters, R.E., Redfern, S.I., Zhang, M., Mao, L., Annex, B.H., et al., 2007. Oxidative phenotype protects myofibers from pathological insults induced by chronic heart failure in mice. American Journal Of Pathology. https://doi.org/10.2353/ajpath.2007.060505.

[65] Bechara, L.R.G., Moreira, J.B.N., Jannig, P.R., Voltarelli, V.A., Dourado, P.M., Vasconcelos, A.R., et al., 2014. NADPH oxidase hyperactivity induces plantaris atrophy in heart failure rats. International Journal of Cardiology. https://doi.org/10.1016/j.ijcard.2014.06.046.

[66] Talbert, E.E., Cuitiño, M.C., Ladner, K.J., Rajasekerea, P.V., Siebert, M., Shakya, R., et al., 2019. Modeling human cancer-induced cachexia. Cell Reports. https://doi.org/10.1016/j.celrep.2019.07.016.

[67] Cray, C., Zaias, J., Altman, N.H., 2009. Acute phase response in animals: a review. Comparative Medicine. https://doi.org/10.1002/ece3.1939.

[68] Mangelsdorf, D.J., Evans, R.M., 1995. The RXR heterodimers and orphan receptors. Cell. https://doi.org/10.1016/0092-8674(95)90200-7.

[69] Evans, R.M., Mangelsdorf, D.J., 2014. Nuclear receptors, RXR, and the big bang. Cell. https://doi.org/10.1016/j.cell.2014.03.012.

[70] Botling, J., Castro, D.S., Öberg, F., Nilsson, K., Perlmann, T., 1997. Retinoic acid receptor/retinoid X receptor heterodimers can be activated through both subunits providing a basis for synergistic transactivation and cellular differentiation. Journal of Biological Chemistry. https://doi.org/10.1074/jbc.272.14.9443.

[71] Shulman, A.I., Mangelsdorf, D.J., 2005. Retinoid X receptor heterodimers in the metabolic syndrome. New England Journal of Medicine. https://doi.org/10.1056/NEJMra043590.

[72] Zhang, W., Ni, P., Mou, C., Zhang, Y., Guo, H., Zhao, T., et al., 2016. Cops2 promotes pluripotency maintenance by stabilizing nanog protein and repressing transcription. Scientific Reports. https://doi.org/10.1038/srep26804.

[73] Svitkina, T., 2018. The actin cytoskeleton and actin-based motility. Cold Spring Harbor Perspectives in Biology. https://doi.org/10.1101/cshperspect.a018267.

[74] Lee, S.H., Dominguez, R., 2010. Regulation of actin cytoskeleton dynamics in cells. Molecules and Cells. https://doi.org/10.1007/s10059-010-0053-8.

[75] Fukawa, T., Yan-Jiang, B.C., Min-Wen, J.C., Jun-Hao, E.T., Huang, D., Qian, C.N., et al., 2016. Excessive fatty acid oxidation induces muscle atrophy in cancer cachexia. Nature Medicine. https://doi.org/10.1038/nm.4093.

[76] He, W.a., Calore, F., Londhe, P., Canella, A., Guttridge, D.C., Croce, C.M., 2014. Microvesicles containing miRNAs promote muscle cell death in cancer cachexia via TLR7. Proceedings of the National Academy of Sciences of the United States of America 111(12):4525–4529. https://doi.org/10.1073/pnas.1402714111.

[77] Guttridge, D.C., 2015. A TGF-β pathway associated with cancer cachexia. Nature Medicine. https://doi.org/10.1038/nm.3988.

[78] Kir, S., White, J.P., Kleiner, S., Kazak, L., Cohen, P., Baracos, V.E., et al., 2014. Tumour-derived PTH-related protein triggers adipose tissue browning and cancer cachexia. Nature 1:1–19. https://doi.org/10.1038/nature13528.

[79] Schäfer, M., Oeing, C.U., Rohm, M., Baysal-Temel, E., Lehmann, L.H., Bauer, R., et al., 2016. Ataxin-10 is part of a cachexokine cocktail triggering cardiac metabolic dysfunction in cancer cachexia. Molecular Metabolism 5(2):67–78. https://doi.org/10.1016/j.molmet.2015.11.004.

[80] Kimura, M., Naito, T., Kenmotsu, H., Taira, T., Wakuda, K., Oyakawa, T., et al., 2014. Prognostic impact of cancer cachexia in patients with advanced non-small cell lung cancer. Supportive Care in Cancer: Official Journal of the Multinational Association of Supportive Care in Cancer, 1699–1708. https://doi.org/10.1007/s00520-014-2534-3.

[81] Yang, L., Wang, J., Li, J., Zhang, H., Guo, S., Yan, M., et al., 2016. Identification of serum biomarkers for gastric cancer diagnosis using a human proteome microarray. Molecular & Cellular Proteomics 15(2):614–623. https://doi.org/10.1074/mcp.M115.051250.

[82] Antunes-Correa, L.M., Nobre, T.S., Groehs, R.V., Alves, M.J.N.N., Fernandes, T., Couto, G.K., et al., 2014. Molecular basis for the improvement in muscle metaboreflex and mechanoreflex control in exercise-trained humans with chronic heart failure. The Australian Journal of Pharmacy: Heart and Circulatory Physiology. https://doi.org/10.1152/ajpheart.00136.2014.

[83] Megeney, L.A., Kablar, B., Garrett, K., Anderson, J.E., Rudnicki, M.A., 1996. MyoD is required for myogenic stem cell function in adult skeletal muscle. Genes & Development 10(10):1173–1183. https://doi.org/10.1101/gad.10.10.1173.

[84] Megeney, L.A., Perry, R.L.S., Lecouter, J.E., Rudnicki, M.A., 1996. bFGF and LIF signaling activates STAT3 in proliferating myoblasts. Developmental Genetics 19(2):139–145. https://doi.org/10.1002/(SICI)1520-6408(1996)19:2<139::AID-DVG5>3.0.CO;2-A.

[85] Townsend, K.L., An, D., Lynes, M.D., Huang, T.L., Zhang, H., Goodyear, L.J., et al., 2013. Increased mitochondrial activity in BMP7-treated Brown adipocytes, due to increased CPT1- and CD36-mediated fatty acid uptake. Antioxidants and Redox Signaling. https://doi.org/10.1089/ars.2012.4536.

[86] De Keijzer, M.H., Brandts, R.W., Brans, P.G.W., 1999. Evaluation of a biosensor for the measurement of lactate in whole blood. Clinical Biochemistry. https://doi.org/10.1016/S0009-9120(98)00105-2.

[87] Alves, C., Melo, C., Almeida, N., Chammas, R., Brum, P., 2017. Metronomic chemotherapy with cisplatin induces skeletal muscle wasting and impairs ubiquitin-proteasome system in B16-F10 tumor-bearing mice. Journal of Muscle Health 1(2):1006.

[88] Perez-Riverol, Y., Csordas, A., Bai, J., Bernal-Llinares, M., Hewapathirana, S., Kundu, D.J., et al., 2019. The PRIDE database and related tools and resources in 2019: improving support for quantification data. Nucleic Acids Research. https://doi.org/10.1093/nar/gky1106.

[89] Cox, J., Matic, I., Hilger, M., Nagaraj, N., Selbach, M., Olsen, J.V., et al., 2009. A practical guide to the maxquant computational platform for silac-based quantitative proteomics. Nature Protocols. https://doi.org/10.1038/nprot.2009.36.

[90] Kil, Y.J., Becker, C., Sandoval, W., Goldberg, D., Bern, M., 2011. Preview: a program for surveying shotgun proteomics tandem mass spectrometry data. Analytical Chemistry. https://doi.org/10.1021/ac200609a.

[91] Jannig, P.R., Moreira, J.B.N., Bechara, L.R.G., Bozi, L.H.M., Bacurau, A.V., Monteiro, A.W.a., et al., 2014. Autophagy signaling in skeletal muscle of infarcted rats. PloS One 9(1):1–12. https://doi.org/10.1371/journal.pone.0085820.

[92] R Development Core Team, R, 2011. R: a language and environment for statistical computing.

[93] Ritchie, M.E., Phipson, B., Wu, D., Hu, Y., Law, C.W., Shi, W., et al., 2015. Limma powers differential expression analyses for RNA-sequencing and microarray studies. Nucleic Acids Research. https://doi.org/10.1093/nar/gkv007.

[94] Carvalho, B.S., Irizarry, R.A., 2010. A framework for oligonucleotide microarray preprocessing. Bioinformatics. https://doi.org/10.1093/bioinformatics/btq431.

[95] Wickham, H., 2016. ggplot2: elegant graphics for data analysis.

